6

Seismogenesis of earthquakes occurring in the ancient rift basin of Kachchh, Western India

BAL KRISHNA RASTOGI, PRANTIK MANDAL, AND SANJIB KUMAR BISWAS

Abstract

This chapter describes the mode of formation and seismogenesis of the very active Mesozoic-age intraplate 200 km × 300 km Kachchh Rift, which continues to be seismically active. As well as aftershocks of the 2001 M_w 7.7 Bhuj earthquake, seismicity has continued to occur to M_w 5.6 levels along other newly activated faults up to a distance of 240 km over the past dozen years. This ongoing activity has provided a natural laboratory for studying seismogenesis of intraplate rifts. Over the past decade, detailed investigations included intense seismicity monitoring with up to 75 broadband seismographs, ground motion detection with a GPS network of 22 stations and InSAR, active fault investigation, and subsurface mapping with various types of geophysical surveys. The results of these studies led to the detection and mapping of subsurface faults. Though the low GPS-derived horizontal deformation (2–5 mm/yr) may be adequate to trigger earthquakes along pre-existing faults away from the rupture zone, pockets of high vertical deformation (1–27 mm/yr) were detected by InSAR, indicating greater vertical deformation. The uplift was possibly aided by migration of the stress pulse due to a 20 MPa stress drop associated with the mainshock. It is inferred that tectonic inversion of the rift is causing uplift of the region. The seismicity and receiver function analysis suggest a thin crust overlying a thinned lithosphere. Tomographic studies reveal the presence of a high-velocity ~100 km wide solid mafic intrusive with embedded low-velocity zones, which suggest the presence of metamorphic fluids or volatile carbon dioxide. The thin crust and lithosphere facilitated placement of mafic intrusive and metamorphic fluids and/or volatile carbon dioxide from the underlying magma chambers. It is inferred that the high-density mafic body acts as a local stress concentrator and the low-velocity fluid-filled patches act as asperities.

Intraplate Earthquakes, ed. Pradeep Talwani. Published by Cambridge University Press.

6.1 Introduction

Large earthquakes are continuously occurring along different faults in the Kachchh intraplate rift basin of Western India. In this chapter we describe geological features and details of the lower crust and upper mantle derived from tomography, receiver function, and shear-wave splitting; we speculate on the cause of stress accumulation; and give details of continuing seismicity triggered after the M_w 7.7 earthquake along nearby faults, possibly caused by a stress pulse, and the unusually high uplift detected by InSAR and GPS.

During the continental breakup of India from Africa in the late Triassic (210 Ma), Western India experienced crustal stretching (thinning) and the formation of three failed rifts of Kachchh (also spelled as Kutch), Cambay, and Narmada. In the Kachchh Rift (KR), magmatic intrusives were emplaced in the lower crust (possibly starting in the late Jurassic, 175 Ma). During the process, several basic intrusive rocks have come up to the surface all over Kachchh (Biswas, 2005). The xenoliths found in these intrusives may have originated in the lower lithosphere and are dated 75 Ma (Sen *et al.*, 2009). The Deccan/Réunion mantle plume during the end of the Cretaceous caused lithosphere thinning and emplaced the Deccan volcanic flood basalt. The KR and the intraplate region in or close to the Deccan Traps has been known to be active for centuries, and many earthquakes have occurred in recent times (inset of Figure 6.1): Koyna (reservoir induced seismicity along with M_w 6.3 in 1967 to M_w 5.6 in 2011) along the Kurdwadi Rift; Latur (1993, M_w 6.2), Jabalpur (1997, M_w 5.8), and Bharuch (1970, M_w 5.4) in the Narmada Rift; and Bhuj (2001, M_w 7.7) in the Kachchh Rift. The 2001 Bhuj earthquake caused 14,000 deaths and destruction in a heavily populated and industrialized region (Rastogi, 2001; Rastogi *et al.*, 2001).

Worldwide intraplate earthquakes, which mainly occur along rifts, are not well understood due to the low level of seismicity. Measuring about 200 km $\times$ 300 km, the Kachchh Rift of Gujarat is seismically one of the most active intraplate regions of the world and has experienced large earthquakes for many centuries and intense seismicity for over a decade. Its six major E–W-trending faults are being reactivated by thrusting. This detailed study of the seismogenesis of the KR has provided insights into understanding intraplate seismicity associated with rift zones.

Large earthquakes and faults in the KR are shown in Figure 6.1. These are: the 1819 M_w 7.8 earthquake along the Allahbund Fault (ABF), the 1845 M_w 6.5 Lakhpat earthquake along the western part of the Kachchh Mainland Fault (KMF), the 1956 M_w 6.0 Anjar earthquake along the Katrol Hill Fault (KHF), the 2001 Bhuj M_w 7.7 earthquake along the eastern extension of the Kachchh Mainland Fault, and the 2006 M_w 5.6 Gedi earthquake along the Gedi Fault (GF).

A seismic reflection survey detected a fault 10 km north of Anjar as part of the KHF along which the 1956 earthquake may have occurred (Sarkar *et al.*, 2007).

Aftershocks of the 2001 Bhuj earthquake of M_w up to 5 have continued for over a decade. Also, several triggered earthquakes of $M_w \leq 5.6$ occurred along different faults in Kachchh up to about 75 km from the mainshock epicenter and also up to 240 km south in Saurashtra, which is a different tectonic province.

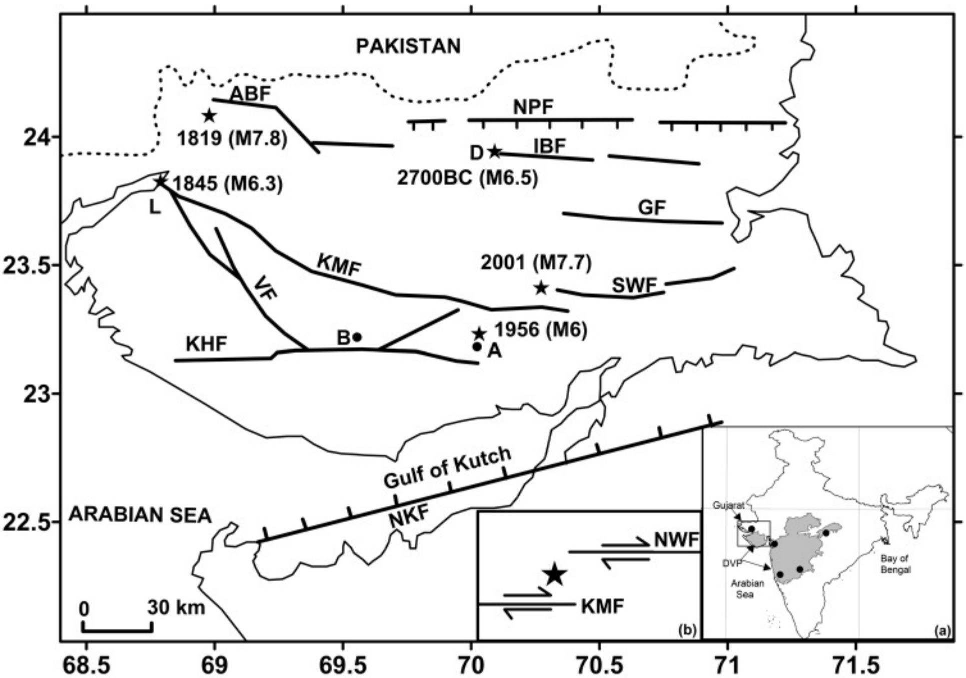

Figure 6.1 Significant earthquakes and their associated faults in Kachchh. Locations are: A, Anjar; B, Bhuj; L, Lakhpat; D, Dholavira. Major faults: ABF, Allah Bund; IBF, Island Belt; KMF, Kachchh Mainland; KHF, Katrol Hill; NPF, Nagar Parkar; NKF, North Kathiawar; VF, Vigodi; GDF, Gora Dungar; BF, Banni; GF, Gedi. The inset diagram (a) shows the Kachchh and Saurashtra area of Gujarat (small square) and the area of the Deccan Traps, along with epicenters of significant earthquakes in Peninsular India. (b) Possible stepover zone between KMF and NWF.

The seismicity over a decade has been monitored with about 75 broadband seismographs. Geodetic deformation has been detected with over 22 permanent GPS stations, 11 campaign GPS stations, and InSAR in and around the aftershock zone. Seismic, gravity, and magnetotelluric measurements have revealed the orientation of faults and information about subsurface structure (Gupta *et al*., 2001; Sarkar *et al*., 2007; ISR Annual Report 2012, isr.gujarat.gov.in). Geological and paleoseismological investigations indicate past activity on faults.

The availability of this large dataset has enabled detailed study for this region. In this chapter, we review the information generated on crustal and upper mantle structure in the source zone of a large paleorift to understand the rift structure and seismogenesis of the intraplate earthquakes occurring in the KR zone. A seismotectonic model of the KR area is presented based on new ideas on structural as well as seismicity patterns, fault mechanisms, and geodetic deformation.

The Indian intraplate region has negligible internal deformation (3 ± 2 mm/yr; Paul *et al*., 2001). However, some areas such as the Narmada Rift have high *in-situ* stress (Gowd *et al*., 1992). Moreover, the large intraplate earthquakes occurring along rifts are located in the lower crust. The presence of a magmatic intrusive body has been inferred for KR lower crust, which may accumulate stress and lead to brittle failure. Some low-velocity patches are found in and around the intrusive, which are speculated to be fluid-filled asperities.

6.2 Tectonic framework, structure, and tectonic evolution of Kachchh Rift basin

6.2.1 Structure and tectonics

The western margin of the Indian plate is the locale of three failed pericratonic rifts formed during the breakup of Gondwanaland involving stretching and thinning of the crust (Biswas, 1987, 2005): the KR formed earliest during the Late Triassic (210 Ma), followed by the Cambay Rift, which formed during the Early Cretaceous, and the Narmada Rift, which formed during the Late Cretaceous. The crust is found to be 35–37 km thick in the KR compared to 38–42 km in the surrounding region (Mandal, 2012a). Rift evolution with syn-rift sedimentation continued through the Jurassic till the Early Cretaceous as the Indian plate separated from Africa and drifted northward along an anticlockwise path. The rift expanded from north to south by successive reactivation of primordial faults of the Mid-Proterozoic Delhi fold belt. The NE–SW strike of the Delhi–Aravalli fold belt swings to E–W in the Kachchh region (Biswas, 1987). The E–W-trending rift basin has a series of E–W-trending faults (Figure 6.2). The KR is bound by the Nagar Parkar uplift on the north and the Kathiawar uplift (Saurashtra horst) on the south, lying along the sub-vertical Nagar Parkar and North Kathiawar faults (NPF and NKF). The rift is styled by three main uplifts (from north to south), Island Belt, Wagad, and Kachchh Mainland, along three intrarift faults, Island Belt (IBF), Kachchh Mainland (KMF), and South Wagad (SWF), with intervening grabens and half-grabens. The Island Belt uplift is a narrow south-tilted basement ridge, which is broken and displaced by tear faults into four separate uplifts described as "islands." The uplifts are upthrust basement blocks tilted along sub-vertical faults with initial normal separation. The structure is characterized by tilted blocks and half-grabens within a south-tilted asymmetric rift basin. The NKF is the bounding master fault along which the rift subsided most. All the faults are sub-vertical, dipping 90° to 75° towards the adjacent half-graben or graben (Biswas, 1987). Blanketing sediments over the basement drape over the tilted edges of the upthrusts as marginal flexures, which are narrow deformation zones along master faults enclosing complicated folds, locally much faulted and intruded by igneous rocks. In the western part the step-faulted uplifts are tilted to the south, with flexures draped over the faulted uplift northern edges (Biswas, 2005). In the eastern part a large uplift, Wagad, occurs between the Mainland and Island Belt uplifts. It is tilted opposite to the north with a narrow deformation zone along the faulted southern edge (Biswas, 2005). The back-slope ends against the Bela horst of the Island Belt uplift. The Mainland and Wagad uplifts occur in *en echelon* pattern. The KMF and SWF are parts of a left-stepping dextral strike-slip fault system (Biswas and Khattri, 2003). The SWF is the eastward continuation of the KMF after side-stepping with an overlap zone between Bhachau and Adhoi. Another important tectonic feature in the KR zone is a subsurface basement ridge – Median High –

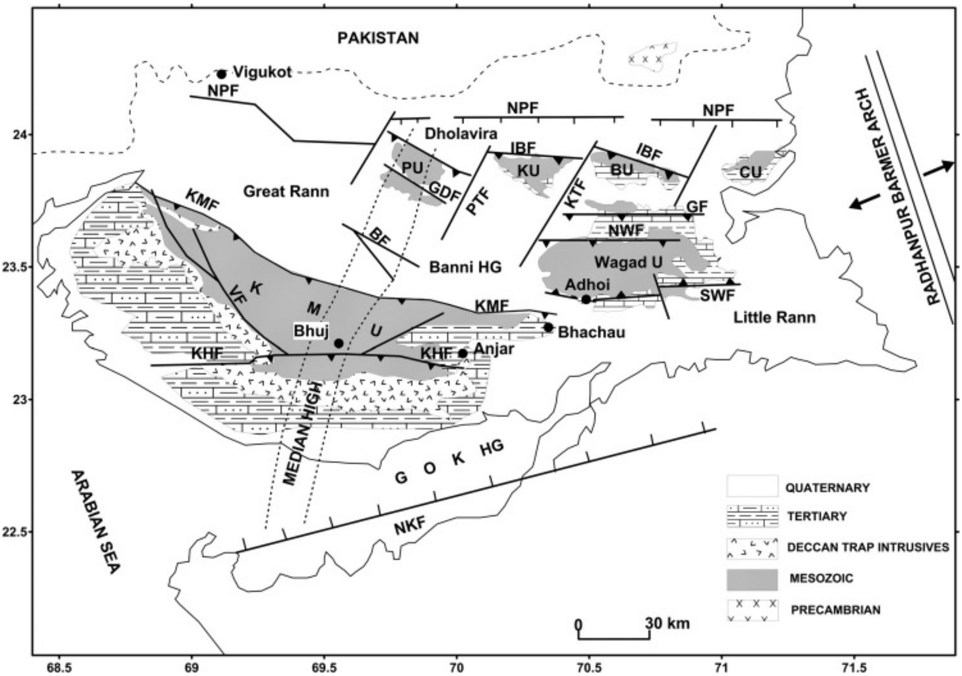

Figure 6.2 Tectonic map of Kachchh (modified after Biswas, 2005). Major faults: ABF, Allah Bund; IBF, Island Belt; KMF, Kachchh Mainland; KHF, Katrol Hill; NPF, Nagar Parkar; NKF, North Kathiawar; VF, Vigodi; GDF, Gora Dungar; BF, Banni; GF: Gedi. Uplifts: PU, Pachham Is.; KU, Khadir Is.; BU, Bela Is.; CU, Chorar Is.; Wagad U, Wagad Uplift; KMU, Kachchh Mainland Uplift. HG, Half-Graben. GOKHG, Gulf of Kutch Half-Graben. ABF is mislabeled near Vigukot.

that crosses the basin at right angles to its axis in the middle. Acting as a hinge it divides the basin into a deeper western part and a shallower and more tectonic eastern part. We also notice that the KR is terminated in the east against a transverse subsurface basement ridge, the Radhanpur arch, which is the western shoulder of the adjacent N–S oriented Cambay rift, and, to the west the KR merges with the offshore shelf.

A south to north depth section (Figure 6.3b) depicts possible dip directions of faults inferred from intensive field work by Biswas (2005), and a modified version based on new seismological and geophysical data is shown in Figure 6.3c. The dip directions of the KMF and SWF inferred by Biswas are towards the north and south, respectively, and opposite to the dip directions inferred by Rastogi. Biswas interprets that the dip directions of the two faults are towards each other, so that the low-lying Samkhiali and Banni grabens may be formed. However, Rastogi opines that the Kachchh Mainland can uplift only along a south-dipping fault while the Wagad can uplift only along a north-dipping fault. Once the uplifts are formed, the area between the two uplifts will be low-lying. Bouguer anomaly data indicate that the basement has not gone down in Samkhiali and Banni with respect to the Wagad and Kachchh Mainland uplifts. From trenching, Morino *et al*. (2008a, b) inferred

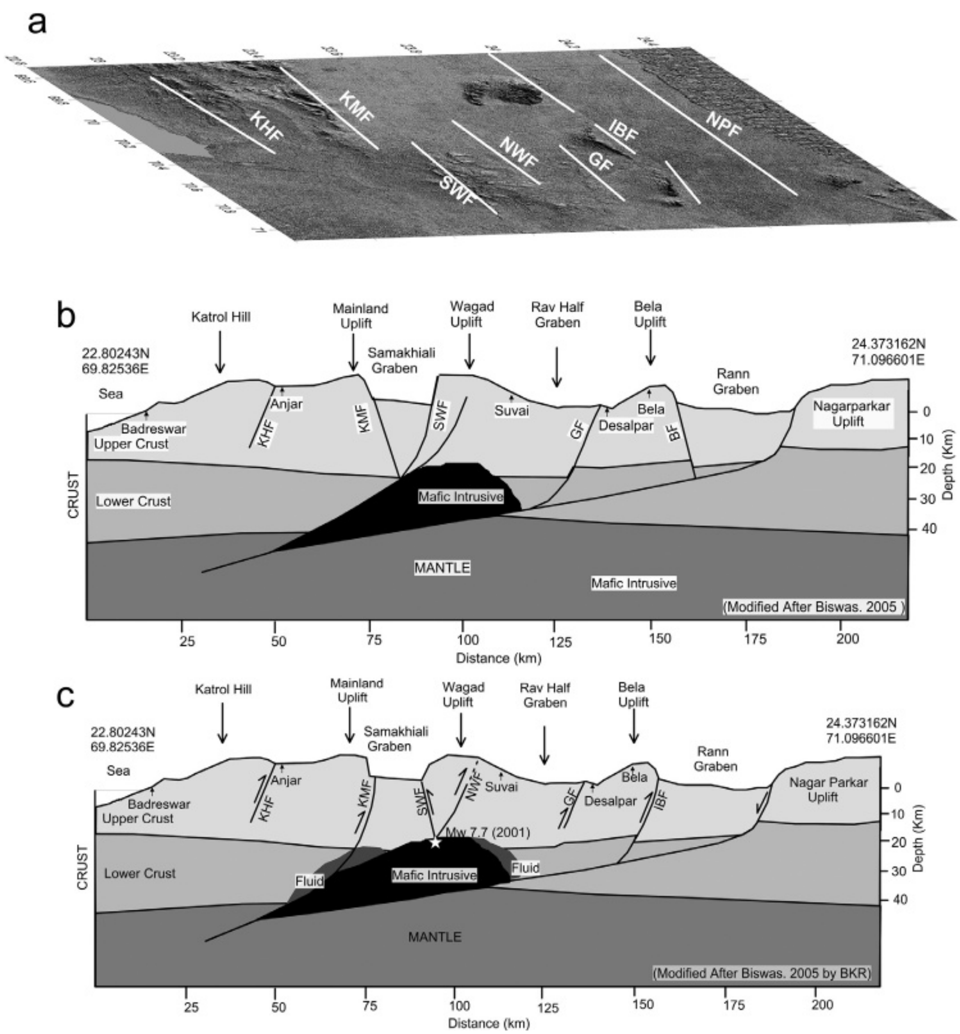

Figure 6.3 (a) DEM and faults in the KR. (b) Depth section across the KR inferred from detailed geological mapping by Biswas (2005) (lower part). (c) Depth section modified based on new geophysical surveys as well as hypocentral depths by Rastogi. The intrusive magmatic body and fluid zones around it are shown.

southward dip of the KMF. The dips given by Rastogi are based on two magnetotelluric profiles, 20 km apart, lying east and west of the epicenter of the 2001 Bhuj earthquake (23° 26.4′ N 70° 18.6′ E, about 15 km northwest of Bhachau) (Mohan *et al*., 2013). The two faults are observed down to at least 12 km depth in the two 22 and 15 km long profiles with station spacing of 1–2 km (Figure 6.4). The surface extension of the NWF would mark the boundary between Mesozoic and Tertiary formations. From the magnetotelluric surveys, the sediments are found to be 1.5 to 2.3 km thick in the Samkhiali basin and 5–6 km in the Wagad

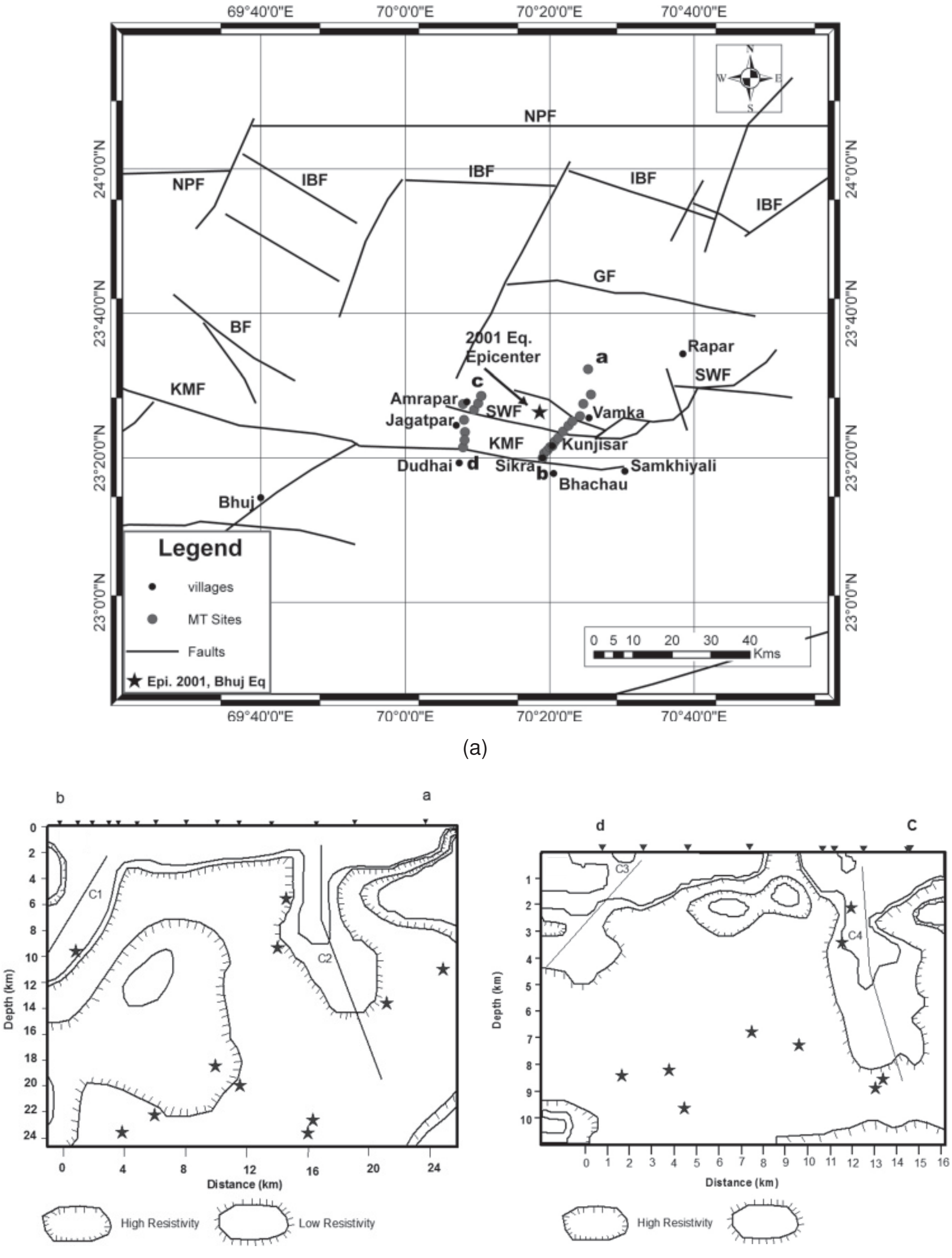

Figure 6.4 (a) Locations of MT profiles ab and cd on Geology and tectonic setting of the area (after Biswas, 2005). Profiles are east and west of the epicenter of the 2001 Bhuj earthquake (23° 26.4′ N 70° 18.6′ E (ISC), which is shown as a star 15 km northwest of Bhachau. (Epicenter by USGS is 9 km WSW.) (b) 2D geoelectric depth section (eastern profile) down to 24 km. The conductive block towards the “b” side is the Kachchh Mainland Block and the conductive block towards the “a” side (around 16 km distance) is the Wagad Block. M ≥ 4 hypocenters from 2006 to 2012 are plotted: C1, KMF; C2, SWF. (c) 2D western geoelectric depth section to 14 km depth. Epicenters of M ≥ 4 from 2006 to 2012 are plotted: C3, KMF; C4, SWF. Low resistivity zones indicate faults.

Uplift area. The Bouguer gravity anomaly also indicates larger sedimentary thickness in Wagad as well as Kachchh Mainland Uplift areas due to gravity lows as compared to high gravity value areas of the Samkhiali basin and Banni area (Singh *et al*., 2013).

Figure 6.3c indicates that the south-dipping hidden NWF is a left step-over fault of the KMF, being separated from it by about 30 km. The step-over zone between Bhachau and Bharudia is a stressed zone of compressive stress (Figure 6.1, inset). The SWF is a conjugate fault to the NWF and intersects it at mid-crust region. The 2001 mainshock originated near this intersection. Such step-over faults have been suggested theoretically by Segall and Pollard (1980) and Sibson (1986), and through an analog sand-box model by McClay and Bonora (2001), and have been mapped in many areas (in Charleston, South Carolina, by Dura-Gomez and Talwani (2009) as well as in the New Madrid seismic zone by Russ (1982), Pratt (2012), and others referred to therein).

6.2.2 Tectono-volcanic events

Tectonic episodes were accompanied by deep crustal magmatic activity (Biswas, 2005; Ray *et al*., 2006; Paul *et al*., 2008; Sen *et al*., 2009). At least two phases of magmatic activity are evident. The first activity took place during the extensional stage when ultramafic rocks intruded into the older Jurassic sediments. Presumably at this time the deep-seated magmatic body was emplaced at the site of the mantle rupture close to the basin center (Biswas, 2005). The second took place during the Late Cretaceous (65 Ma) post-rift uplift stage when plume-related alkali and tholeiitic basalts were intruded into the younger Early Cretaceous sediments and extruded as the Deccan Trap flows. The volcanic activity was associated with thinning of the sub-Kutch lithosphere. Mandal (2010) found that the lithospheric thickness varies from 62 to 63 km in the KR and from 65 to 77 km in the surrounding region. The rifting started in the Late Triassic–Early Jurassic and continued through the Deccan volcanism in the Early Cretaceous (Biswas, 1987). The bulk of the Kutch alkalic lavas came from an Indian Ridge mantle source rather than the Réunion plume. The Kutch lithosphere was composed of spinel lherzolite that was largely converted to spinel wehrlite by carbonatite metasomatism. Such carbonatite melts were generated by decompression melting of the asthenosphere during its rise to shallower levels in response to extension and thinning of the lithosphere. Mantle xenolith-bearing alkalic magmas were mainly generated from a mixture dominated by asthenospheric material and the edge of the Deccan/Réunion plume. These melts ascended, while picking up xenoliths, along pathways created by deep rift faults. Tholeiites may have come from elsewhere in the south as plumelets, from the hotter part of the Deccan plume head (Sen *et al*., 2009).

6.2.3 Tectonic evolution and existing earthquake generation models of the Kachchh Rift zone

Rifting was aborted by the trailing edge uplift during the Late Cretaceous pre-collision stage of the Indian plate, when the leading edge of the plate was slab-pulled towards the Tethyan trench (Biswas, 2005). The uplift caused structural inversion during the rift–drift transition stage, when most of the uplifts with drape folding over the edges came into existence by upthrusting of the basement domino blocks along the master faults. This created first-order marginal flexures over the foothill uplifts. Lateral motion during the drift stage of the plate induced horizontal stress and near-vertical normal faults, which were reactivated as reverse faults during initiation of the inversion cycle, and became strike-slip faults involving divergent oblique-slip movements (Biswas, 2005). The present structural style evolved by right-lateral slip, which shifted the uplifts progressively eastward relative to each other from south to north. This resulted in the present *en echelon* positioning of the uplifts with respect to the Kutch Mainland uplift. The strike-slip related structural changes modified the linear flexures, breaking them into individual folds at the restraining and releasing bends. Narrow deformation zones complicated by second-order folds and conjugate Riedel faults formed along the master faults, modifying the initial drape folds (Biswas, 2005). Syntectonic intrusions further modified the shape and geometry of the individual second-order structures. Igneous rocks extensively intruded the Mesozoic sediments during rifting followed by post-rift hotspots related to Deccan volcanism (Sen *et al*., 2009). Studies of the intrusive rocks and seismological data suggest the presence of mafic/ultramafic magmatic bodies close to the crust–mantle boundary (Mandal and Pujol, 2006; Mandal and Chadha, 2008; Mandal and Pandey, 2010).

Inversion continued during the post-collision compressive stress regime of the Indian plate and the KR basin became a shear zone with transpressional strike-slip movements (with thrusting at depth) along the active sub-parallel rift faults (Biswas, 2005). The same tectonic phase is continuing, as evident from neotectonic movements along these faults that are responsible for the present first-order geomorphic features and seismicity. In the current tectonic cycle, under N–S compressive stresses, the NWF and SWF are the most active faults, as evident from the concentration of aftershock hypocenters in the overlap zone (Biswas, 2005; Mandal and Horton, 2007). Pulses of movement along these faults are responsible for generation of new fault fractures within the respective deformation zones. These new fractures are propagating through the recent piedmont and scarp-fan sediments in the frontal zones of the thrusts, as seen in the trenches dug close to the KMF and KHF (Malik *et al*., 2008; Morino *et al.*, 2008a, b) and in GPR surveys. The morphotectonic features also indicate Quaternary uplift along the above-mentioned master faults (Malik *et al*., 2008).

During the present compressive stage, the Radhanpur arch acts as a stress barrier for eastward movements along the principal deformation zones, which is creating additional strain in this part of the basin between the arch and the Median High (Biswas, 2005). Towards the eastern end of the Mainland uplift, the right lateral KMF becomes the SWF by left-stepping with an overlap in the region between Samakhiali and Lakadiya (Biswas, 2005). This stepover zone – formed initially as the Samakhiali–Lakadiya graben – is presently a convergent transfer zone undergoing transpressional stress in the strained eastern part of the basin. This is the most strained part of the basin. Expectedly, this is the most favored site for rupture nucleation. The occurrence of the 2001 Bhuj quake (M_w 7.7) in

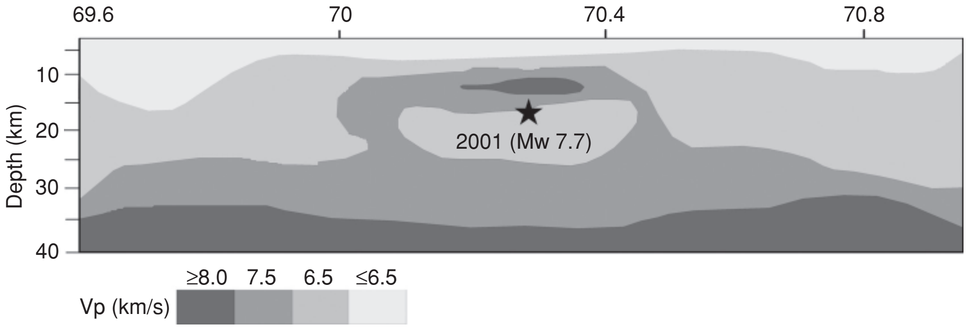

Figure 6.5 Cartoon displaying Vp distribution with depth along an E–W profile through the 2001 Bhuj earthquake epicenter. The hypocenter of the 2001 mainshock projected on this line lies in a low-velocity patch. The outer portion of the intrusive body also has low-velocity fluid-filled zones. For color version, see Plates section.

this zone and the concentration of aftershock hypocenters around it further validate this conclusion.

Aftershock data suggest a reverse slip on a fault plane (NWF) dipping 40–60° to the south as the causative fault for repeated earthquake nucleation (Mandal and Horton, 2007). Continued continental compression and repeated thrusting generate fractures related to the main fault-forming highly stressed fault zone, which seems to be the zone of repeated earthquake nucleation (Biswas, 2005). This earthquake nucleation zone is defined by several subsidiary faults branching off the main KMF. The causative fault, the NWF (North Wagad Fault), of the Bhuj 2001 earthquake seems to be one such fault that lies north of it. The occurrence of the 2001 Bhuj earthquake has been explained in terms of large local stress perturbations associated with the pre-existing fault intersection (with respect to favorably optimally oriented maximum horizontal stress direction) and mafic crustal intrusive bodies below the KR zone (Gangopadhyay and Talwani, 2003; Mandal and Pandey, 2010). The presence of faults transverse to the NWF may lead to large stress concentrations in the lower-crustal magmatic layer (at 14–34 km depth), thereby, the favored zone of earthquake nucleation (Mandal and Pandey, 2010). Presumably, the fluid released by the eclogitization of olivine-rich lower-crustal rocks aids the slippage along this causative fault and hence the occurrence of the 2001 Bhuj earthquake sequence (Mandal and Pandey, 2010; Mandal, 2011; Mandal, 2012a, b).

6.2.4 Identification of magmatic intrusive bodies

The P and S tomography results (Mandal *et al.*, 2004a) suggest the presence of a regional high-velocity, low Poisson's ratio body around the 2001 mainshock epicenter with a head extending 60 km in the N–S direction and 40 km in the E–W direction at 10–25 km depth (Figure 6.5), which may be a mafic intrusive of the rifting stage. At deeper depths it may be larger. It has been speculated that this body is causing stress build-up. Its velocity is inferred to be high (Vp: 7.15–8.11 km/s) at 24–42 km depth and density 3.06–3.37 g/cm^3

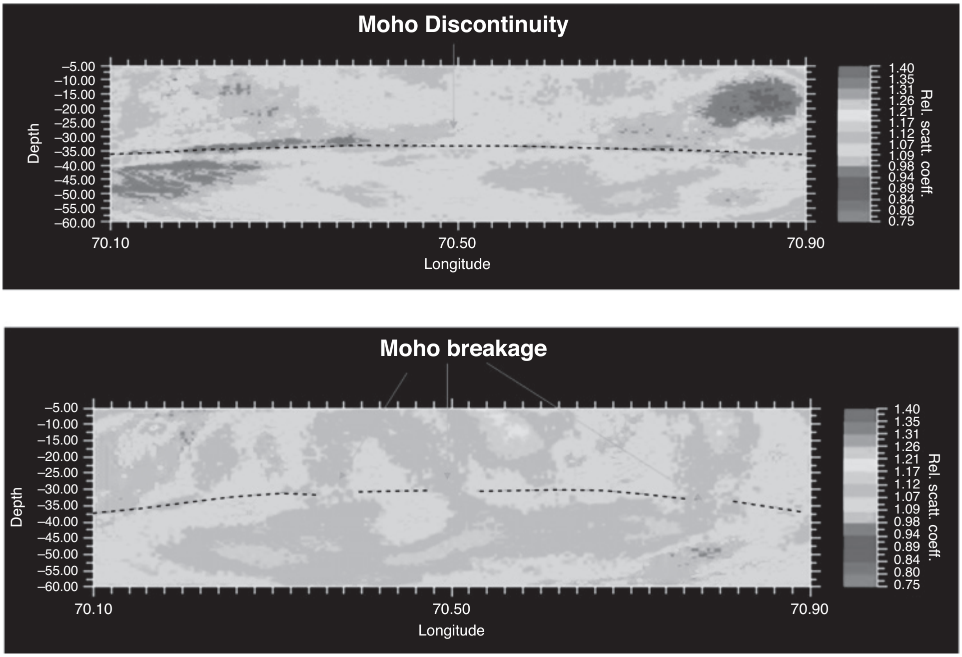

Figure 6.6 (Upper part) Intact Moho in the Kachchh region 70 km north of the epicenter of the 2001 Bhuj earthquake. (Lower part) Disturbed Moho at the 23.3° N latitude of the 2001 Bhuj earthquake. The profile length is 90 km. For color version, see Plates section.

as estimated according to the formula, ρ (g/cm^3) = 0.32 Vp (km/s) + 0.77 (Mandal and Pandey, 2010).

Due to magmatic intrusion, the Moho is likely to be broken, disturbed, and/or scattered. This is revealed by 3D Q-structure in the epicentral zone of the 2001 earthquake in Kachchh at a depth of around 40 km (Figure 6.6; Sharma *et al*., 2008) but intact Moho north of the epicentral zone.

Such magmatic intrusives have been inferred for the Narmada Rift (Rajendran and Rajendran, 1998) and most of the worldwide rifts that act as stress concentrators and cause deepening of the brittle–ductile transition depth (Mukherjee, 1942; Mooney *et al*., 1983; Mechie *et al*., 1994; Prodehl *et al*., 1994; Johnston, 1994, 1996; Mooney and Christensen, 1994; Nyblade and Langston, 1995; Liu and Zoback, 1997; Singh *et al*., 1999; Kumar *et al*., 2000; Deverchere *et al*., 2001; Kruger *et al*., 2002; Manglik and Singh, 2002; Wilson *et al*., 2003; Gao *et al*., 2004).

The KR has a large-scale presence of alkaline rocks and mantle xenoliths at subsurface depths in the form of plugs, cones, and sheet-like bodies containing olivine, opx, cpx, and spinel (Karmalkar *et al*., 2000, 2008; Desai *et al*., 2004; Sen *et al.,* 2009). Melts for such alkaline rocks are reportedly generated by the partial melting of carbon dioxide-rich lherzolite (Sen *et al*., 2009). Eclogitization or serpentinization of these may release carbon dioxide. The availability of such sources of melts is assured by the thin crust and lithosphere.

6.2.5 Low-velocity fluid-filled zones in and around magmatic bodies in the lower crust

Mandal *et al*. (2004a) detected a low-velocity high Poisson's ratio zone within the mafic body at the hypocentral depth of the mainshock ($\sim$18–25 km), which is inferred to be a fluid-filled fractured rock mass and which might have acted as an asperity for generation of the 2001 Bhuj earthquake (Figure 6.5). From further detailed work on Vp and Vs tomography, Mandal and Chadha (2008) inferred several low-velocity patches (Figure 6.7). From 3D mapping of b-values (Mandal and Rastogi, 2005; Singh *et al*., 2011; Nagabhushan Rao, 2012), a high b-value ($\sim$1) zone is found to be sandwiched within the maximum rupture zone at depths of 15–25 km with a low b-value (0.6 to 0.8) above and below. In the same zone Mishra and Zhao (2003) and Singh *et al*. (2012) found low Vp and Vs, high crack density, porosity, saturation rate and Poisson's ratio, and suggest the presence of a fluid-filled and fractured rock matrix.

Such a low-velocity fluid zone was inferred by Kato *et al*. (2009) from high-resolution 3D tomography around solidified intrusive bodies in the intraplate eastern margin of the Japan Sea back-arc basin, and they attributed the large earthquakes of the area to the presence of an intrusive body and fluids around it. It is speculated that the trapped aqueous fluids resulted from metamorphism or were released from degassing of mantle magmatic material or volatiles such as carbon dioxide (Zhao *et al*., 1996; Miller *et al*., 2004; Wang and Zhao, 2006; Mandal and Pandey, 2010).

6.2.6 Paleoseismological investigations

Based on Baker's (1846) leveling survey, Bilham (1999) inferred 11 m slip (uplift and subsidence) along the Allahbund fault due to the 1819 earthquake. The inferred fault is north-dipping with possibly listric fault geometry, with a steep dip at shallow depth but a gentle dip at larger depth. Rajendran (2000) estimated lesser uplift of 4.3 m and suggested a growing fold at shallow depths along a north-dipping thrust (Rajendran and Rajendran, 2001). From radiocarbon age data of liquefaction features they suggested occurrence of a previous earthquake 800–1000 years ago and suggested the ABF to have been previously active, as a historic event was possible in AD 893 (Rajendran and Rajendran, 2002, 2003). At Dholavira in northern Kachchh the archeological evidence indicates an earthquake during the closing decades of stage III of the settlement (2500–2200 BC) (Singh, 1996; Rajendran and Rajendran, 2003; Kovach *et al*., 2010). Bisht (2011) suggests that this event occurred during 2100–2000 BC and identifies two earlier earthquakes also during stage II (2900 BC) and stage III (2700 BC).

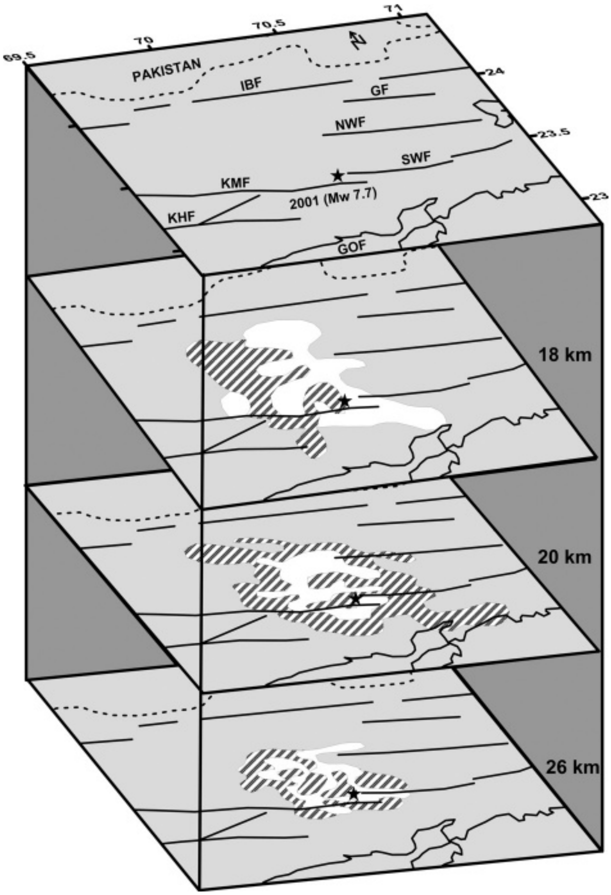

Figure 6.7 Schematic 3D model displaying Vp distribution with depth. The 2001 Bhuj earthquake hypocenter (22 km value most accepted, but ranges from 22 to 26 km) shown by a star lies on the boundary of low- and high-velocity patches. The hatched areas are low-velocity zones while the white areas mark the high-velocity zones. At a depth of 34 km (not shown) the low-velocity zone is much larger.

The ABF, KMF, SWF, IBF, and KHF are found to be active by Quaternary movements as observed in trenches (Figure 6.8; Rajendran and Rajendran, 2002, 2003; Malik *et al.*, 2008; Morino *et al.*, 2008a, b and www.isr.gujarat.gov.in/Annual Reports 2009–10, 2010–11, 2011–12). This indicates that different faults are active neotectonically. Below we describe the work of the Institute of Seismological Research (ISR), most of which was done with Malik and Morino.

The deformation zone of the 1819 Allahbund earthquake of Kachchh was mapped with a precise elevation survey in an area 80 km long and 6–7 km wide. The amount of uplift measured in 2007 is up to 5.8 m. By adding 1.8 m estimated erosion since 1819, a total uplift of 7.6 m is estimated for the 1819 earthquake. The Allahbund fault is interpreted to

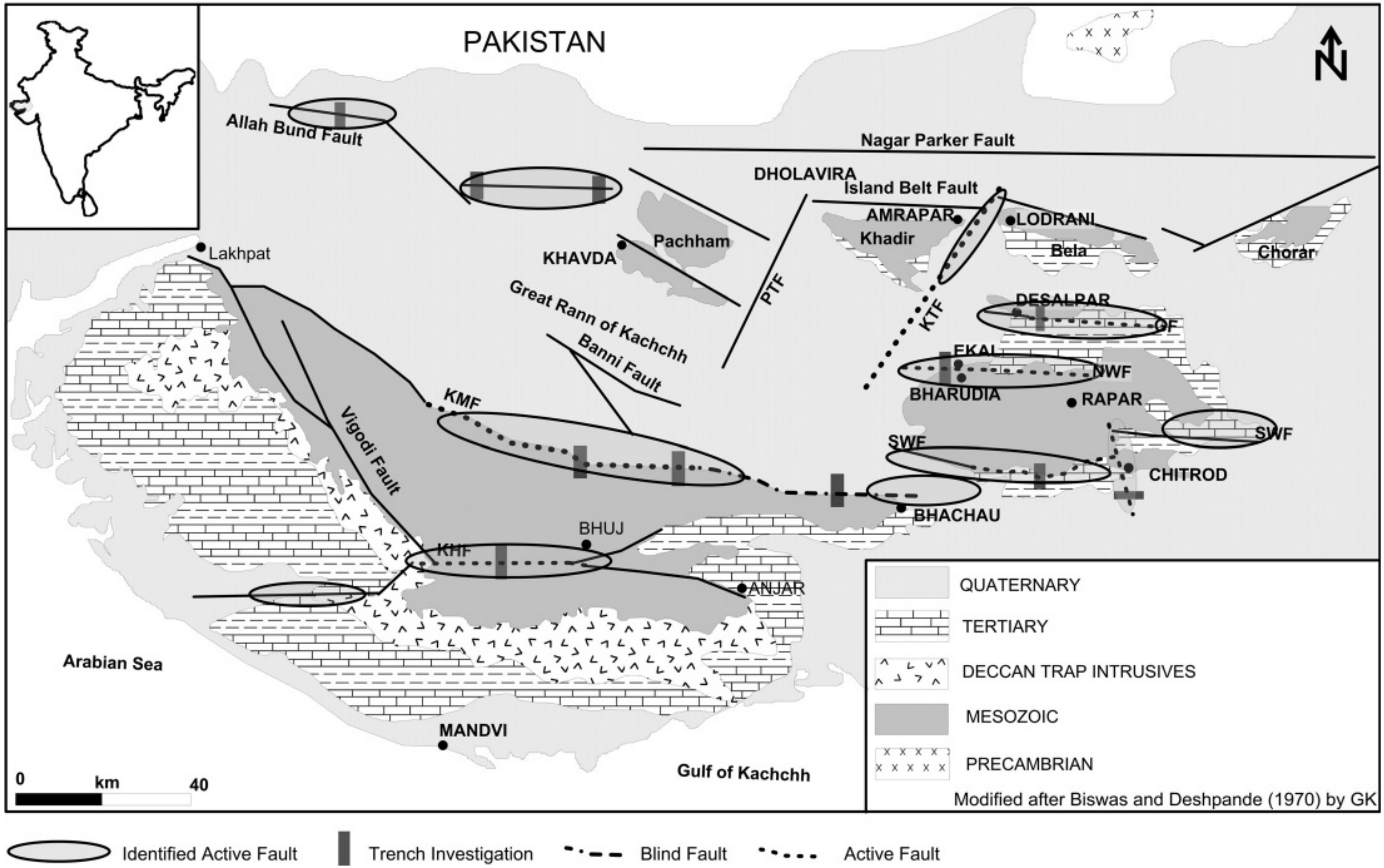

Figure 6.8 Active fault map of Kachchh by ISR prepared with data from 27 shallow trenches. The portions of faults where trenching has revealed active movements are marked with ellipses.

be north-dipping. At Vigukot, 10 km north of Allahbund, three large and three or four small events are inferred based on sand craters and disrupted human settlements found in trenches.

The presence of tidal deposits in the Sindri lake area indicates that the sea has receded by 100 km from here to the present position. In the eastern part of the ABF near Karimsahi, several trenches and uplift of paleochannels reveal uplift during the last few thousand years. Due to uplift, the paleochannels could have been formed at 3–4 ka and again uplifted by 2 m at 2 ka, as revealed by OSL dating of samples at different elevations. A trench near Dharamshala indicates three events in the last 3 ka. Along a streamcut nearby, a highly deformed zone was identified. OSL dates indicate that a 3 ka bed has thrust over a 2.7 ka bed.

The KMF is found to be south-dipping in a trench at Jhura in the central part of the KMF, where a cumulative deformation of 5 m has been assessed as due to three events. The two last events had 70 cm slip each. A rough estimate of the age of formations is 5 ka, as determined by the optically stimulated luminescence method. At Lodai, in the eastern part of the KMF, the two large events show slips of 33 cm and 40 cm during the late Pleistocene to Holocene period and older events along two older faults show a cumulative slip of 98 cm. The Mesozoic rocks override Quaternary along a south-dipping fault. Identification of a pressure ridge by remote sensing and thorough ground checks helped in identifying the activity in this part of the KMF. Further east, there is cumulative slip of 4 m in the Quaternary, and the last event at an inferred age of 2 ka indicates a 50 cm slip.

In a trench at Wandhey in the central part of the KHF, Quaternary deformation indicates three large events during the late Holocene to a few ka along three fault strands, which displaced the older terrace deposits comprising sand, silt, and gravel units along with overlying younger deposits from units 1 to 5 made of gravel, sand, and silt.

In the Wagad area, the slips noticed for events possibly in the past few ka are: the Gedi fault along a rivercut shows slip of 1 m; along the South Wagad fault two events are noticed with slips of 30 cm and 50 cm along two fault strands in a trench in the Adhoi anticline at 3–4 ka; south of the Wagad area, in the Samkhiali basin, slip of 75 cm is measured in a trench.

6.3 Seismicity of Gujarat state

Figure 6.9 shows significant faults and epicenters of about 200 mainshocks of magnitude ≥ 2 from 1684 to 2000 in Gujarat and the adjoining region bound by 20°–25.5° N and 68°–75° E. Table 6.1 shows the magnitude distribution of mainshocks during the pre- and post-2001 periods (Rastogi *et al.*, 2013a).

About 200 km × 300 km, Kachchh is seismically one of the most active intraplate regions of the world. It has six major E–W-trending faults of the failed Mesozoic rift, which are being reactivated by thrusting. Prior to the 2001 M_w 7.7 Bhuj earthquake, Kachchh had experienced three large earthquakes: 1819 M_w 7.8 Allah Bund (24.00° N 69.00° E), 1845 M_w 6.3 Lakhpat (23.80° N 68.90° E), and 1956 M_w 6 Anjar (23.30° N 70.00° E). Some large earthquakes have been documented based on archeoseismology, such as the Dholavira earthquake (Bisht, 1997, 2011), but these earthquakes occurred along different faults (Figure 6.1). The second seismic region in Gujarat is the Narmada Rift zone, which

Table 6.1 *Magnitude distribution of mainshocks in Gujarat from 1684 to 2012*

M/Year	2–2.9	3–3.9	4–4.9	5–5.9	6–6.9	≥7	Total
1668–2000	11	79	62	27	2	1	183
2001–2012	17	26	14	6	—	1	63

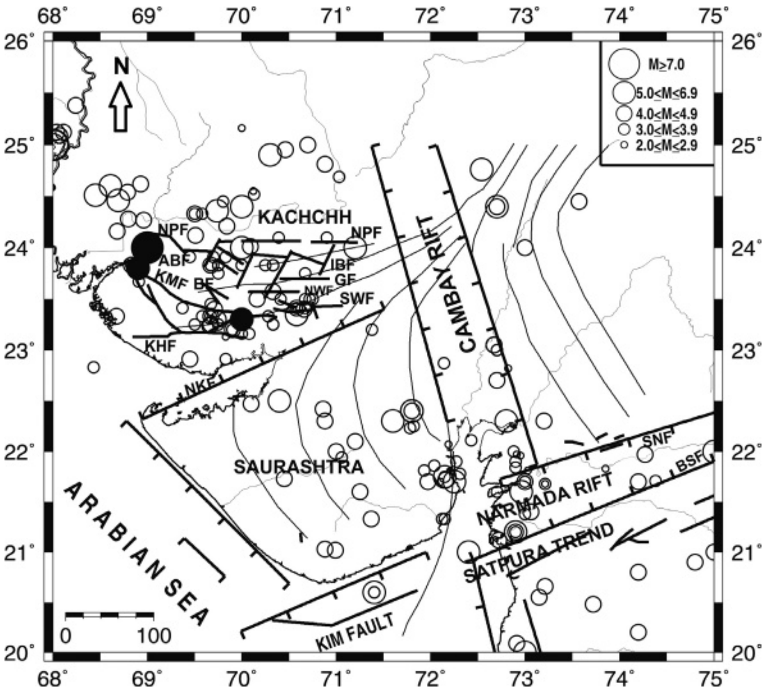

Figure 6.9 Significant faults and epicenters of earthquakes of magnitude ≥ 2 from 1684 to 2000 excluding aftershocks in Gujarat. Filled circles are the three significant events in Kachchh of 1819, 1845, and 1956. The Proterozoic-age Aravali trend branches off in three directions. In Kachchh it becomes E–W, along which faults might have formed.

experienced the severely damaging 1970 Bharuch earthquake of M_w 5.4 at its western end and larger earthquakes further east, including 1927 M_w 6.3 Son, 1938 M_w 6.5 Satpura, and 1997 M_w 5.8 Jabalpur events. The third seismic zone consists of the Cambay basin, east and southeast of Kachchh, and the Saurashtra Peninsula, south of Kachchh, which has experienced seismicity of magnitude less than 6.

Seismic networks have been operating since 1976 and earthquakes of magnitude ≥3.5 are routinely located. Most of Gujarat having been heavily populated for centuries, it is expected that for the past 200 years no earthquake of magnitude ≥4 has been missed, as such earthquakes are felt strongly over wide areas. Their locations may have an accuracy of

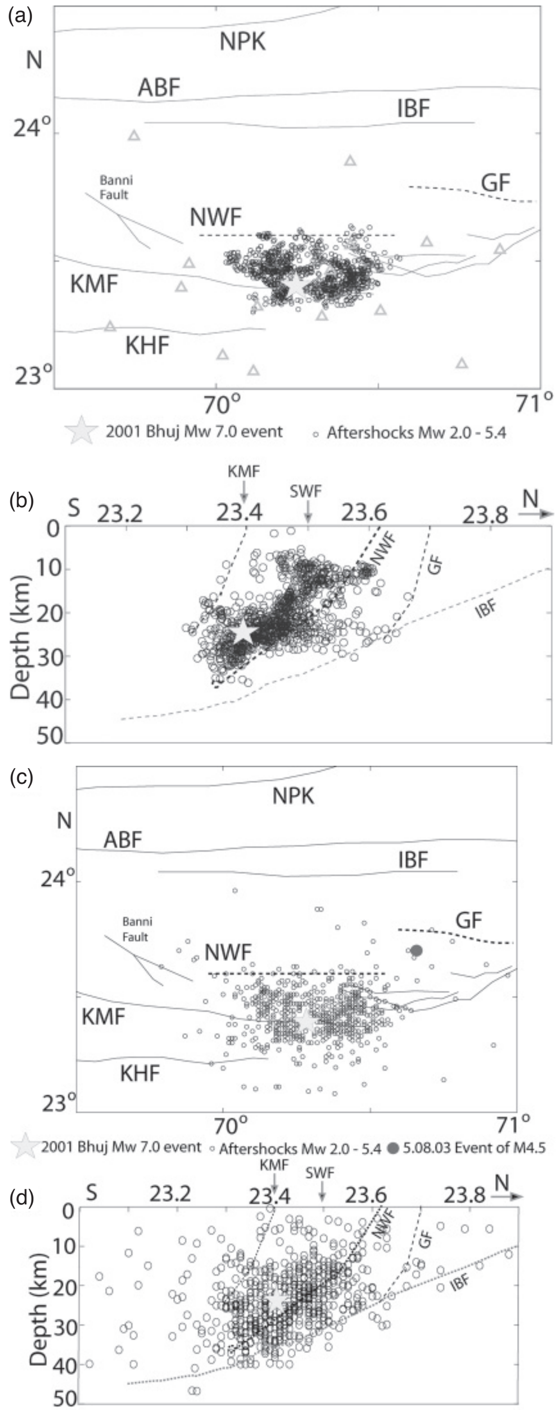

Figure 6.10 (a) Epicenters and (b) foci of Kachchh earthquakes during 2001 show that they were confined to the NWF and 40 km × 40 km area. (c) Epicenters and (d) foci of Kachchh earthquakes during the two years 2002 to 2003. A few faults near the NWF became slightly active (NGRI data): Nagar Parkar (NPF), Allah Bund (ABF), Island Belt (IBF), Gedi (GF), South Wagad (SWF), Kachchh Mainland (KMF) and Katrol Hill (KHF).

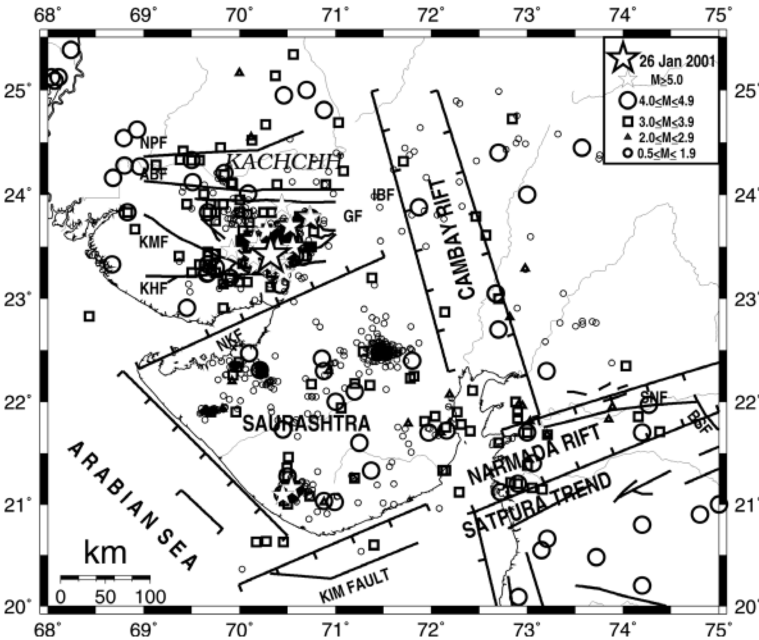

Figure 6.11 Epicenters of earthquakes in Gujarat during 2001–12. The epicenters of shocks of M < 2.0 are mostly in areas of intense local monitoring.

10–15 km. The six shocks of $M_w \geq 5.0$ and about 25 strongly felt (M_w 3 to 4.9) earthquakes that occurred in the decade after 2000 are very well located.

6.3.1 Seismicity with time in Kachchh and the nature of seismic sources

Starting in 2001, up to 75 broadband seismographs have been operating in Gujarat (500 km × 600 km), of which some 40 are in Kachchh. During 2001 to 2003, the aftershocks of the 2001 Bhuj earthquake were confined to the main rupture zone of 40 km × 40 km area north of the KMF and along an inferred hidden North Wagad fault (Figure 6.10). During 2001 to 2012 some 10,000 $M_w \geq 0.5$ shocks were located in Gujarat (Figure 6.11).

Aftershocks of the 2001 Bhuj earthquake to $M_w \sim 5$ level have continued for over a decade, including 16 $M_w \geq 5$, 250 $M_w \geq 4$, about 4000 $M_w \geq 3$ events, and some 5000 other well-located shocks of M_w 1.0 to 2.9 (Mandal and Rastogi, 2005; Mandal *et al.*, 2007; Rastogi *et al.*, 2013a, b). Up to 2003 there were 15 aftershocks of $M_w \geq 5$ and one in 2006. The latest significant aftershock was of M_w 4.9 on March 9, 2008.

6.3.2 Orientation of faults and depth of the seismogenic zone in Kachchh

The parameters of the 2001 mainshock are: 23.419° N, 70.232° E, focal depth 16 km (USGS). Some other depth estimates are 22 km or 23 km (ISC; Antolik and Dreger, 2003).

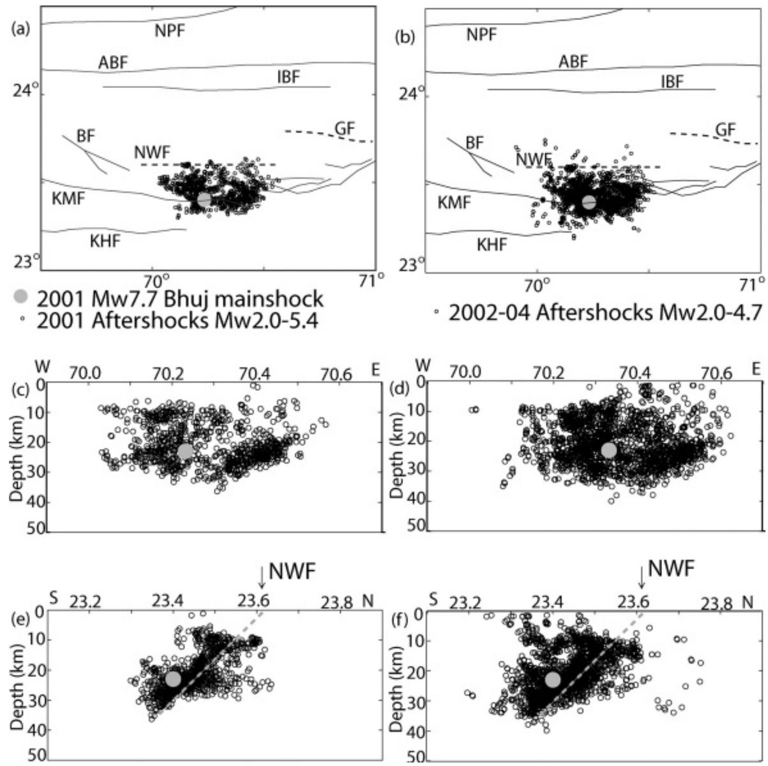

Figure 6.12 (a) HypoDD relocations of 1402 aftershocks of M_w 2.0–5.4 during 2001. Large circle marks the location of the 2001 Bhuj mainshock. (b) Epicenters of aftershocks during 2002–4. (c) E–W depth plot of relocated aftershocks during 2001. (d) E–W depth plot of relocated aftershocks during 2002–4. (e) N–S depth plot of relocated aftershocks during 2001. (f) N–S depth plot of relocated aftershocks during 2002–4.

Yagi and Kikuchi (2001, eri.u-Tokyo.ac.jp) determined source duration of 20 s, and fault dip 58°. Rupture with maximum slip of 8.5 m propagated mostly towards the west for 40 km, with a small slip towards the east for 20 km along the fault width from 8 km below the surface to 35 km depth along the NWF. If projected onto the surface, this would be about 60 km × 30 km in area between the KMF and NWF lying between 23° 20′ and 23° 34′ N, 69° 50′ and 70° 20′ E, which we take as the main rupture zone. The eastern end of the rupture zone terminates north of Bhachau. Antolik and Dreger (2003) have given a similar rupture model.

The epicenters of the mainshocks, foreshocks, and aftershocks during 2001 to 2009 and depth sections are shown in Figure 6.12 (Mandal and Pandey, 2010; Mandal, 2012b). The hypocenters were first determined using the Hypo71 program with up to 56 P and S phases with accuracy of better than 0.5 km horizontal and 1.0 km in depth (Rastogi *et al.*, 2013a). The subsurface orientation of seismogenic faults and depth of the seismogenic zone in the

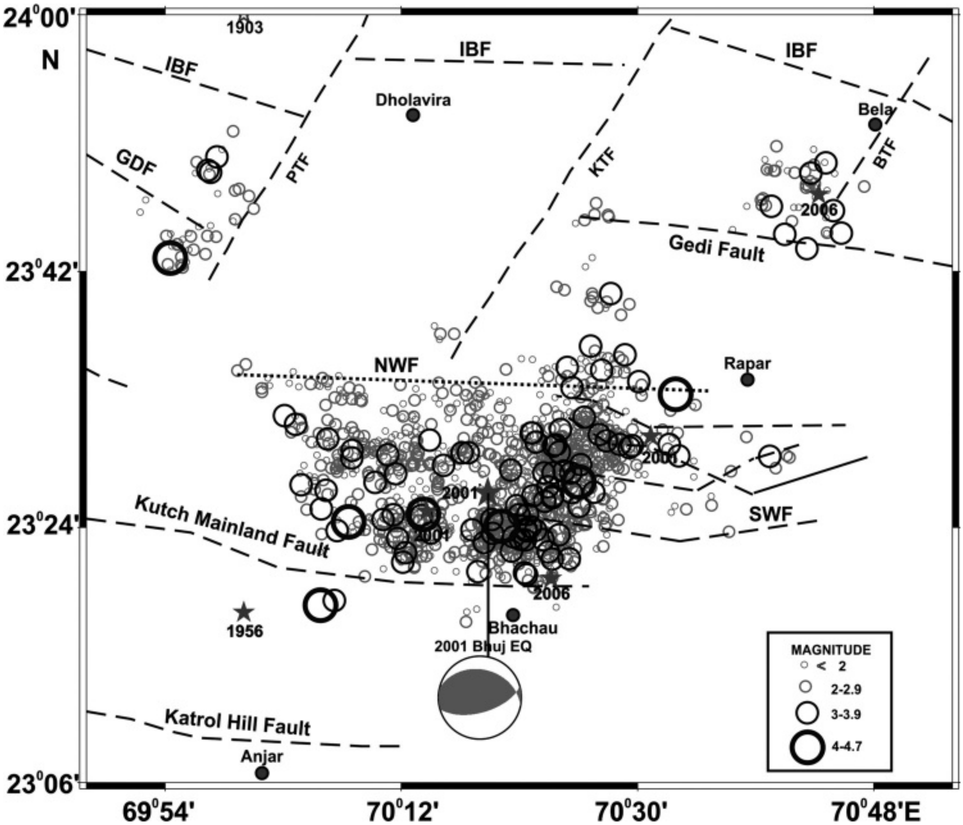

Figure 6.13 Results of HypoDD clustering analysis of the Hypo71 locations during 2007–11 in Kachchh [Kutch] (modified after Rastogi *et al*., 2013b). Epicenters of earthquakes of M ≥ 5 are shown by stars.The North Wagad, Gedi, and Gora Dungar faults show clear concentrations. The Suvai transverse fault also shows a concentration of epicenters. Activity was seen along the Khadir Transverse Fault (KTF) along which an M_w 5.1 earthquake occurred on June 19, 2012, with a long aftershock sequence. East of it and about 20 km west of Rapar, a concentration of several shocks north of the NWF defines a N–S-trending transverse fault, as in the previous figure. A few shocks of M_w < 4.7 have occurred south of the KMF since 2006. As these are at shallow depths, they are inferred to be associated with the KMF and association with the NWF is ruled out. For color version, see Plates section.

aftershock zone of the 2001 earthquake, as well as nearby activated faults, was obtained using precise relocations by double-difference (HypoDD). The hypocentral plots depict the NWF being active from 8 to 35 km depth and the Gedi fault (GF) to 12 km depth. The HypoDD plot for the period January 2007 to May 2011 (Rastogi *et al*., 2012) indicates clustering along the NWF and GF, and for the sequence of October 28, 2009, an M_w 4.6 earthquake along Gora Dungar Fault and some concentration along the Khadir transverse fault (Figure 6.13).

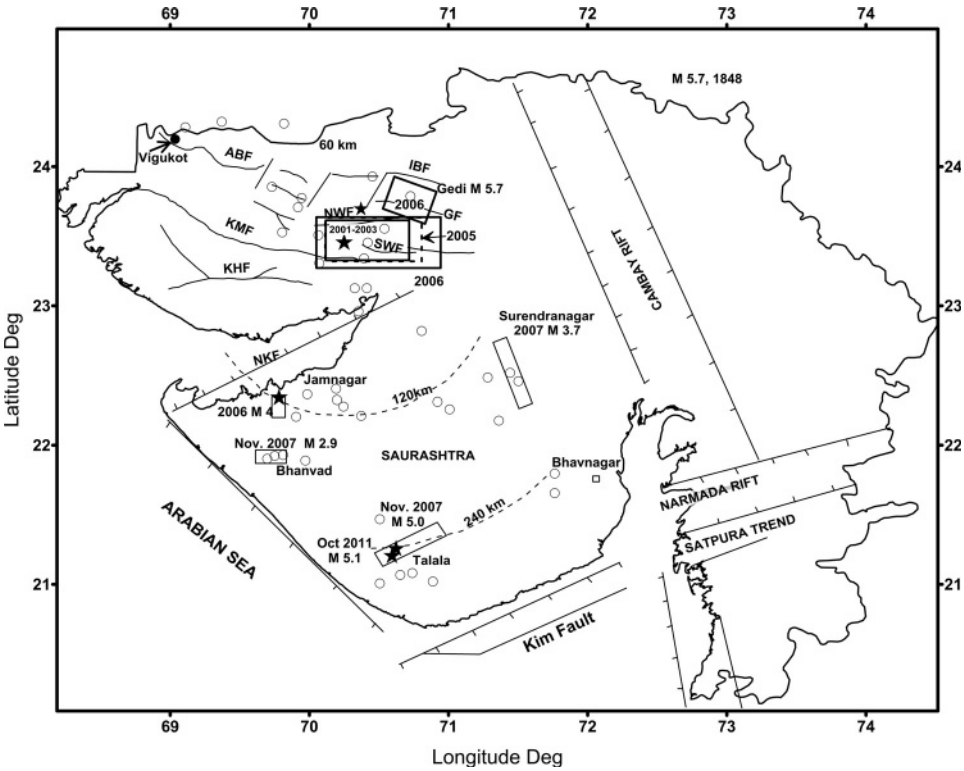

Figure 6.14 Long-time and delayed triggering of seismicity in Gujarat from 2006 to 2011. Epicentral zones for significant sequences are marked by rectangles. The seismicity migrated 120 km south to the Jamnagar and Surendranagar area and as far as 240 km in the Talala area of Saurashtra.

6.4 Long-distance delayed triggering of shocks in Gujarat after the 2001 M_w 7.7 Bhuj earthquake due to stress pulse migration

6.4.1 Triggered seismicity in Kachchh and Saurashtra

Around the aftershock zone of the M_w 7.7 Bhuj earthquake of 2001, several mainshocks of M_w 3–5.6 occurred along different faults up to distances of 75 km away during 2006–12 (Figure 6.14). Initially, the seismicity spread eastward to the SWF, but then to other faults from 2006. These faults include the KMF, IBF, GDF, SWF, and GF. The total number of such mainshocks is at least 20 (Table 6.2) in Kachchh. Many of these mainshocks are associated with foreshock–aftershock sequences, e.g., M_w 5.6 earthquake in March 2006 along the GF about 75 km northeast of the 2001 mainshock epicenter, M_w 4.4 shock of October 28, 2009, along the Gora Dungar fault, and M_w 5.1 shock of June 19, 2012, along a transverse fault north of the 2001 rupture zone (Figure 6.14 and Table 6.2). Table 6.3 compares felt and damaging earthquakes in Kachchh for the pre-2001 (200 yr) and 2001–12 periods.

Table 6.2 *Mainshocks in Kachchh after the 2001 Bhuj earthquake along different faults, and other than aftershocks along the NWF.* M_w *until April 2006 from NGRI and subsequently from ISR. Many of these are associated with their own foreshocks and aftershocks. USGS magnitudes are usually* m_b

SN	Y	M	D	Lat.	Long.	Dep. km	Mag. M_w	Mag. USGS	Location	Mechanism
	2001	1	26	23.44	70.31	16.0	7.7	7.7	18 km NW of Bhachau North Wagad F.	Thrust
1	2004	1	8	23.91	70.90	20.0	4.2		Gedi/Is. Belt F.	
2	2004	6	7	23.87	70.15	29.4	4.2		Dholavira/Is. Belt F.	
3	2005	3	8	23.85	69.74	11.6	4.3		Gora Dungar F.	
4	2005	10	8	23.35	70.69	24.0	4.5		South Wagad F.	
5	2005	10	9	23.74	69.93	6.6	4.3		Gora Dungar F.	
6	2006	2	03	23.92	70.44	28.0	5.0	4.5	Gedi F., foreshock	Thrust
7	2006	3	07	23.79	70.73	3.0	5.6	5.5	Tr. Bela F./Gedi F., ms	Left lateral
8	2006	4	06	23.78	70.74	3.0	4.8	5.0	Gedi F., aftershock	Thrust
9	2006	4	06	23.34	70.39	29	5.6	5.5	Lakadia, SWF	
10	2006	4	10	23.51	70.06	4.9	4.9	4.9	* Banni	
11	2006	6	12	23.88	70.43	27.3	4.4		Gedi/Is. Belt F.	
12	2007	5	13	23.44	70.42	20.4	4.7		South Wagad F.	
13	2007	5	24	23.298	70.026	9.0	4.1		Kachchh Mainland F.	Thrust
14	2007	10	8	23.295	70.075	9.6	4.7	4.5	Kachchh Mainland F.	Left lateral
15	2007	12	15	24.03	69.87	15.0	3.7		Allahbund F.	Right lateral
16	2008	3	9	23.396	70.359	18.5	4.9	4.5	South Wagad F.	Left lateral
17	2008	4	4	23.00	70.36	11.1	2.6		**Kandla	
18	2008	7	5	23.53	69.8	8.9	3.3		Banni F.	
19	2009	10	28	23.71	69.91	8.5	4.4	4.4	Gora Dungar F.	Left lateral
20	2011	1	18	23.27	70.51		3.8		Samkhiyali, SWF	
21	2011	5	17	23.55	70.57	18.2	4.2		E. of North Wagad F.	Thrust
22	2011	8	13	23.45	70.40	22.2	4.5	4.3	South Wagad F.	
23	2011	9	27	23.12	70.31	38.0	3.0		**Kandla	
24	2012	4	14	23.39	70.54	19	4.1	4.0	South Wagad F.	
25	2012	6	19	23.65	70.28	11	5.0	5.0	Khadir Tr. F.	
26	2012	12	8	23.13	70.42	21	4.5	4.1	20 km SSE of Bhachau, **Kandla	
27	2013	3	30	23.56	70.38	24	4.5		*Chobari	

* May be aftershock of 2001 Bhuj earthquake.

** May be regional shock as it is single event.

Table 6.3 *Felt and damaging earthquakes in Kachchh. Post 2001, the shocks are mostly aftershocks, but 27 earthquakes of* M_w ~ *3 to 5.6 are independent mainshocks, many of which are associated with foreshocks and aftershocks.*

Mag.	No. of shocks in Kachchh Pre-2001 (200 yr)	No. of shocks in Kachchh 2001–2012
3.5–3.9	46	671
4.0–4.9	25	268
≥5.0	11	21

Moreover, seismicity (M_w 3 to 5.1) has been triggered along small faults at 20 locations up to 120 km south since 2006 and up to 240 km south since 2007 in the Saurashtra region. The three significant sequences that have continued for 5 years with hundreds of felt shocks are (i) near Jamnagar with M_w maximum 4.0; (ii) near Surendranagar with M_w maximum 3.9; and (iii) at Talala with M_w maximum 5 in 2007, M_w maximum 5.1 in 2011 and several M_w 4 to 4.8 tremors (Figure 6.14). The shocks are usually shallow (focal depth < 10 km) and are accompanied by subterranean sounds. The generation of an unusually large number of mainshocks is inferred to be due to triggering caused by migration of the stress pulse generated by the 20 MPa stress drop of the M_w 7.7 earthquake in 2001 to distances of 100–200 km and even 6–8 years after the great earthquake. The triggered seismicity may be due to an increase in Coulomb stress of up to 1 bar in Kachchh and 0.1 bar in Saurashtra, as estimated by viscoelastic modeling (Rastogi *et al.*, 2013b). Added to this may be the major stress from a stress pulse due to the 20 MPa stress drop. Scholz (1977) explained the Haicheng earthquake prediction by propagation of the deformation front at a rate of 110 km/yr. He also quoted such rates of 80 to 270 km/yr (Mogi, 1968) and explained that this may result from stress pulse migration through the mantle (Savage, 1971; Bott and Dean, 1973).

6.4.2 Coulomb stress change

Postseismic Coulomb stress changes (in bars) during 2001 at the surface due to the M_w 7.7 Bhuj 2001 earthquake have been calculated using the Yagi and Kikuchi variable slip model at 15 km depth (crust is considered elastic and mantle viscoelastic). The maximum stress change is 12 bars while a rise of 1 bar extends up to 100 km (Figure 6.15a; Mandal *et al.*, 2007; Choudhury *et al.*, 2013b).

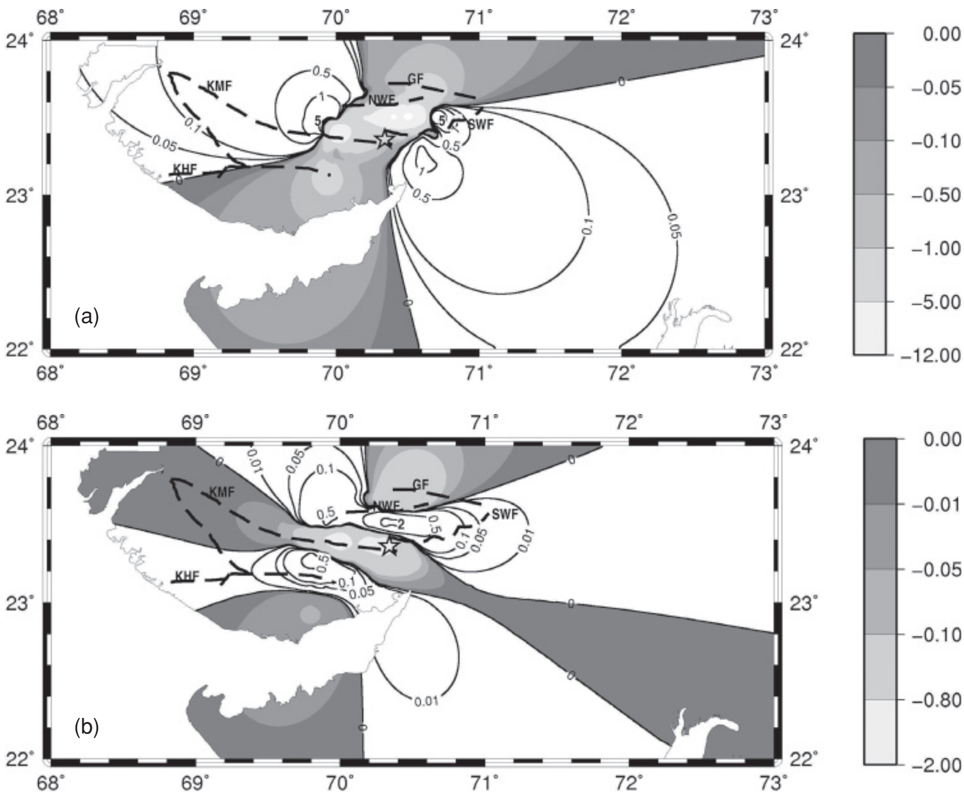

Figure 6.15 (a) Postseismic Coulomb stress changes (in bars) calculated assuming variable slip at 15 km depth due to the M_w 7.7 Bhuj 2001 earthquake soon after the earthquake (2001 mainshock epicenter is marked as a star and negative Coulomb stress areas are shaded). Maximum stress change is 12 bars while a rise of 1 bar extends up to 100 km. (b) Six years after the earthquake. Aftershocks and triggered earthquakes (during 2006–12) have occurred in the zones of positive stress change up to a distance of 75 km in Kachchh along the SWF in the east and the IBF and some other faults in the north, as well as up to 240 km south in Saurashtra. Positive Coulomb stress contours are numbered while negative Coulomb stress contours are shaded (Choudhury *et al*., 2012).

The Coulomb stress during 2006 estimated by considering the viscoelastic process (Rastogi *et al*., 2013b) is shown in Figure 6.15b. After 6 years the Coulomb stress remains positive towards the western part of the IBF (where a few earthquakes other than aftershocks occurred during 2006–12 along the IBF and Gora Dungar Fault) and negative along the eastern part of the IBF as well as around the KMF. It changes to positive towards the SWF and south of the KMF (maximum positive 2 bars), where seismicity that is not aftershocks was triggered from 2006 onwards. Some mainshocks, e.g., 2006 M_w 5.6 along the Gedi Fault and M_w 5.1 on June 19, 2012, north of the NWF, have occurred in the negative zone of Coulomb stress. This indicates the influence of the stress pulse in these areas.

6.4.3 Geodetic observations in Kachchh

Starting in 2006, ISR operates up to 22 permanent differential GPS stations across geological faults in Gujarat. Some 11 campaign stations in Kachchh are occupied bi-annually. Processing is done with 1 mm/yr accuracy (Choudhury *et al.*, 2013a). Local deformation has been estimated with respect to Gandhinagar station, operating more than 200 km east of the epicenter of the main earthquake of 2001. The Indian Institute of Geomagnetism operated two GPS close to two of the ISR stations during 2001–5. Combining the two datasets, the composite plot for the period 2001–9 indicates that near the epicenter the postseismic relaxation was initially large, being 12, 6, 3, and 4 mm for four consecutive 6-month periods of 2001–2, but subsequently reduced (Figure 6.16). Since 2007 all the ISR stations in Kachchh indicate the horizontal deformation to be low, i.e., of the order of 2–5 ± 1 mm/yr. Nevertheless, the horizontal deformation gives a significant strain of 0.05 µs/yr, even as late as 2008–11 (Dumka and Rastogi, 2013; Choudhury *et al.*, 2013b), triggering earthquakes along the SWF (Figure 6.16 inset). However, vertical deformation is found to be quite large, i.e., 2–13 ± 3 mm/yr, as observed by GPS measurements near the epicenter of the 2001 mainshock and up to 75 km north and northeast, being 13 mm/yr at Dholavira and 10 mm/yr at Dudhai during 2006–11 (Rastogi *et al.*, 2012) (Table 6.4).

The interferogram generated with Differential Interferometric Synthetic Aperture Radar (DInSAR) using the ENVISAT ASAR datasets of June 22, 2008 and October 25, 2009, with a baseline separation of 125 m in the area up to 75 km north of the mainshock epicenter (Figure 6.17; Rastogi *et al.*, 2012) indicates vertical deformation rates of 7–27 mm/yr.

Uplift of 16–27 mm/yr was detected along two faults (KMF and KHF) up to 50 km south of the epicenter, measurements of which were done during 2004–7 using ENVISAT ASAR datasets and during 2007–10 using ALOS PALSAR data (Choudhury *et al.*, 2012; Sreejith and Rastogi, 2013).

6.4.4 Cause of triggered earthquakes

We propose, based on the seismological data, that the viscoelastic process and rheologic changes appear to be the plausible causes of the long-distance and delayed triggering of earthquakes with diffusion rates of 5–30 km/yr, which might have also been facilitated by the migration of a stress pulse of 20 MPa stress drop caused by the 2001 M_w 7.7 earthquake. The rate of transmission of the stress pulse (Figure 6.11), considering the seismic area involved, matches a seismogenic permeability of 0.5 to 5 m^2/s (Talwani *et al.*, 2007) suggesting fluid pressure diffusion. Vertical deformation is observed to be high: measured as up to 13 mm/yr by 6 years of GPS observations and 10–27 mm/yr by 10 years of InSAR observations. We suggest that the transmission of the stress pulse into the upper crust could have resulted in vertical deformation as observed in GPS and InSAR measurements.

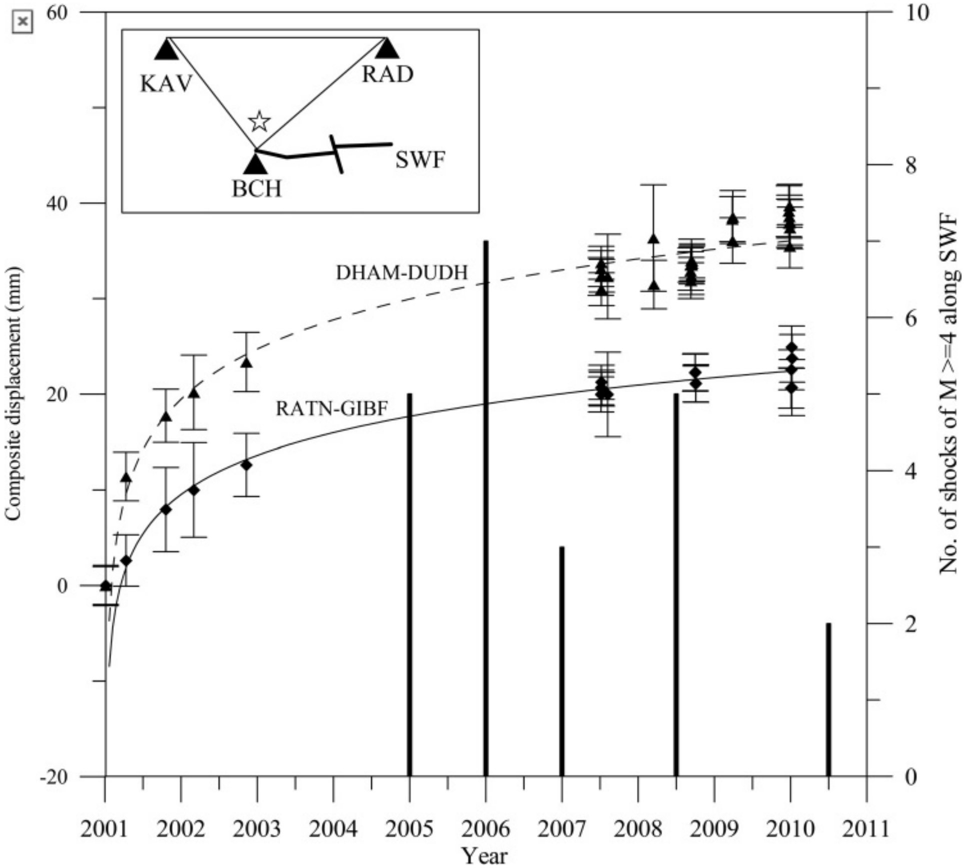

Figure 6.16 Composite map of resultant displacement of two GPS sites (DHAM-DUDH (upper curve) and RATN-GIBF (lower curve) plotted with respect to ISRG from 14 days to 8 years after the 2001 Bhuj earthquake. DHAM and RATN are two GPS stations of Reddy and Sunil (2008) co-located with DUDH and GIBF of the ISR stations, respectively. The displacement decay rate for the upper curve is $D = 7.6 \ln(t) + 20.36$, for the lower curve $D = 5.8 \ln(t) + 10.22$. The number of shocks of $M_w \geq 4$ along the SWF are also shown. The strain calculated in the Kachchh region during 2008–11 along the baselines, as shown in the inset, is representative of the strain in most parts of the active area. For 2005–7 the strain is likely to be greater than that for the period 2008–11 due to the larger displacements.

6.5 Focal mechanism studies

The focal mechanisms for nine significant events (M_w 4.0–5.6) by full waveform moment tensor inversion (10–20 s) reveal a dominant reverse movement with minor strike-slip component on the south-dipping NWF, indicating continued thrusting in the 2001 rupture zone. The 2006 mainshock of M_w 5.6 on the Gedi fault reveals a left-lateral strike-slip movement on an almost vertical fault, but the two aftershocks of M 4–5 indicate a greater thrust component (Mandal *et al.*, 2009; Nagabhushana Rao, 2012). It appears that the

Table 6.4 *High vertical deformations at four GPS campaign stations*

Campaign GPS station	Lat. Long.	Location	Local uplift
Dudhai	23.238N 70.145E	West of 2001 epicenter	10 ± 3 mm/yr
Gadadha	23.867N 70.373E	Close to Dholavira and 30 km north of the 2001 rupture zone	13 ± 3 mm/yr
Lilpar	23.526N 70.636E	NE of 2001 mainshock epicenter	6 ± 3 mm/yr
Fatehgadh	23.683N 70.864E	NE of 2001 mainshock epicenter	5 ± 3 mm/yr

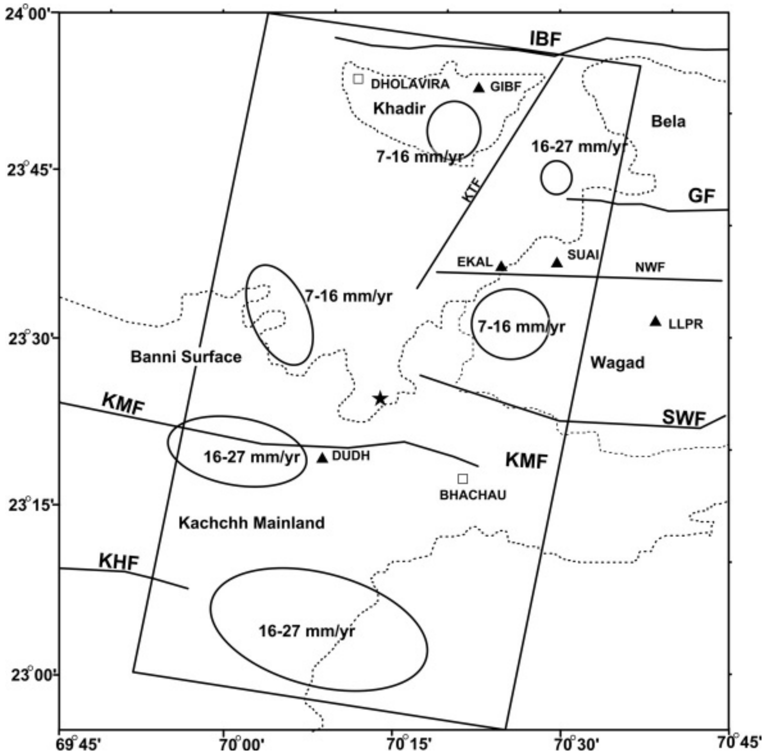

Figure 6.17 Star indicates the 2001 Bhuj earthquake. Local uplifts estimated from interferogram fringes of DInSAR data are shown north of the epicenter. ENVISAT data between two dates 1.5 yr apart (June 22, 2008–October 25, 2009) have been used. North of the epicenter the interferogram fringes were identifiable in hilly uplifted areas only, not in large low-lying areas. South of the epicenter around the KMF and KHF, ENVISAT data were used during 2004–7 and ALOS data, 2007–10 (modified after Choudhury *et al.*, 2012). Deformation could be measured for time intervals of ≥1 yr.

thrusting is along the E–W-trending Gedi Fault and strike-slip is along a northeast-trending conjugate transverse fault. The M_w 5.1 of June 19, 2012 along the Khadir transverse fault indicates left-lateral strike-slip faulting.

Moment tensor focal mechanism solutions of $M > 4$ earthquakes in Kachchh during 2001–10 for a few earthquakes along the Gora Dungar, Kachchh Mainland, and South Wagad faults, surrounding the 2001 rupture zone and believed to have been triggered since 2006, indicate strike-slip. The focal depths are around 3 km for the Gedi and South Wagad earthquakes, 8 km for the Gora Dungar earthquake, and 12 km for the Kachchh Mainland fault earthquake. The focal depths of earthquakes showing thrust mechanisms in the 2001 rupture zone are usually deeper than 10 km. It confirms the view that there could be strike-slip at shallow near-surface depths and thrusting at deeper than 10 km.

Stress inversion using focal mechanism data from five areas across the main rupture zone reveal a N–S orientation of maximum compressive stress with 7–32° rotation, which is attributed to the sizable local horizontal stress component associated with the crustal intrusive bodies in the main rupture zone (Mandal, 2008).

6.6 Results and discussion

The normal faults of the Mesozoic Kachchh Rift were reactivated after the continent–continent collision (40 Ma) in the form of transpressional faults (with thrusting at depth) as inferred from detailed geological field work (Biswas, 2005). New seismological and geophysical data reveal the southward dip of the Kachchh Mainland fault and northward dip of the South Wagad fault, along which large uplifted areas have been formed. Until 2000, seismicity in the region was considered low but with high hazard potential because of historical records of the destruction of Dholavira in 2700 BC due to an earthquake of estimated M_w 6.5, the 1819 Allahbund earthquake of M_w 7.8, the 1845 Lakhpat earthquake of M_w 6.3, and the 1956 Anjar earthquake of M_w 6. These earthquakes occurred along different faults. The picture of low seismicity changed after the 2001 Bhuj earthquake. The KR has been associated with over a decade of aftershock activity of $M_w \geq 5$ and triggering of ~20 earthquakes of M_w 4–5.7 along different large and small faults at up to 75 km distance in a decade. GPS measurements, which started soon after the January 2001 earthquake, revealed 12 mm horizontal displacement for the first 6-month period. It reduced to 6, 3, and 4 mm in the next three 6-month periods. Initially large horizontal displacements favor a shear deformation mode of aftershocks. However, occurrence of M_w 4–5.6 earthquakes, despite small horizontal displacements of 2–5 mm/yr across different faults, was suggested to be due to a stress pulse. The stress pulse is transferred, causing earthquakes along the pre-existing critically stressed faults. Large vertical deformation of up to 13 mm/yr was estimated by GPS for 2006–9 and 10–27 mm/yr from InSAR studies for 2008–9 north of the KMF, and during 2004–7 as well as 2007–10 south of the KMF.

We speculate that the lower crust has a mafic intrusive with high seismic wave velocities, which acts as a stress concentrator. The low-velocity patches at 14–34 km depths indicate the presence of fluids or volatile carbon dioxide, which may act as asperity zones and along which large earthquakes are associated. The presence of patches of partial melt below the lithosphere–asthenosphere boundary (LAB) suggested from receiver function analysis in the central Kachchh Rift zone may be imprints of the Deccan mantle plume (65 Ma) beneath the region (Sen *et al.*, 2009; Mandal, 2010). These may provide compressed carbon dioxide or favorable circumstances for eclogitization and consequent release of fluid, either or both of which facilitate the occurrence of earthquakes. Thin crust and lithosphere provide easy access to the magma source.

Large spatial variations in Vp (from –10 to 13%), Vs (from –11 to 13%), and Vp/Vs ratio up to 1.6 to 1.8 are seen in the main rupture zone of the 2001 Bhuj earthquake at 6–34 km depth, where the tomography model is fairly sampled by the aftershock data (Mandal and Chadha, 2008). At shallower depth (0–10 km) the low Vp, low Vs, and high Vp/Vs could indicate the presence of soft sediments with higher water content.

The aqueous fluid or volatiles containing carbon dioxide are released from the eclogitization of olivine-rich lower crustal rocks. The presence of 2 weight percent carbon dioxide fluid components is suggested in the crystalline basement rocks of the 1993 Latur earthquake (Pandey *et al.*, 2009). Interestingly, John and Schenk (2006) suggest, based on petrologic analysis of eclogites, that, once rupture begins in gabbroic crustal rocks, frictional melting can promote intermediate-to-lower crustal depth earthquakes under eclogite facies conditions and this seismic event can produce permeabilities for external fluids. Thus, the eclogitization of lower crustal olivine-rich gabbroic rocks can provide aqueous fluids or gaseous fluids (such as carbon dioxide and nitrogen) in the intermediate to lower crust. Besides, strong attenuation of seismic waves (low coda Qc) and shear-wave splitting were reported in the Bhuj aftershock zone, which could be explained in terms of the presence of fluids, cracks, or both in the fault zone (Mandal *et al.*, 2004b; Mandal, 2009; Padhy and Crampin, 2006).

Mandal (2012a) finds the crust (35 km) and lithosphere (62 to 63 km) to be thin in the central part of the KR, as compared to 40–42 km thick crust and 65–77 km thick lithosphere in the outer parts of the KR, due to updoming of the lithosphere and asthenosphere (∼6–12 km). Mandal finds a decrease of Vs at 62–77 km depth over an area of 130 km × 90 km, which may indicate the presence of patches of partial melt below the LAB in the central Kachchh rift zone as a remnant of the Deccan mantle plume (65 Ma) beneath the region. Further support for this model is given by the rift axis parallel azimuthal anisotropy, with a delay of 1.6 s evaluated from the SKS splitting study, which is attributed to anisotropy induced by the rift-parallel flows within the 76 ± 6 km thick lithosphere and anisotropy associated with the rift-parallel pockets of partial melts in the asthenosphere, inherited from the plume–lithosphere interaction during the Deccan/Réunion plume episode (∼65 Ma) (Mandal, 2011). Thus, there is a possibility that these patches of partial melts could provide a high input of volatiles containing carbon dioxide into the lower crust. If so, this would contribute significantly to seismo-genesis and continued aftershock activity in the intracontinental Kachchh rift zone.

6.7 Conclusions

The Kachchh rift consists of a network of conjugate faults, some of which extend to large depths. Activity on these faults has produced a series of horsts and grabens, some of which have been leveled by erosion or filled by deposition. The 2001 mainshock that occurred along a hidden North Wagad fault triggered seismicity on adjoining faults by a stress pulse.

New seismological and geophysical data have revealed the subsurface orientations of some active faults. Frequent large earthquakes up to M_w 7.8 have occurred along different faults in the past 200 years. The 2001 Bhuj earthquake has been associated with over a decade of aftershock activity of M_w up to ~6. In addition to that, about 20 earthquakes of $M_w \sim 4$–5.6 were triggered along different large and small faults up to 75 km away in Kachchh. The large vertical displacements of up to 13 mm/yr detected from GPS and 10–27 mm/yr detected from InSAR studies are contributing more to strain build-up than the 2–5 mm/yr small horizontal displacements measured from GPS network and campaign stations. There are some earthquakes that may be triggered in the zones of positive Coulomb stress but some earthquakes are in the negative Coulomb stress zone. Earthquakes 8–10 years after the mainshock, away from the rupture zone and also in the negative Coulomb stress zones indicate that the stress due to a viscoelastic process and/or rheologic process subsequent to the 2001 mainshock adds to the stress due to plate tectonics to cause triggering of earthquakes.

High-velocity mafic intrusives inferred in the lower crust may act as stress concentrators. The postulated low-velocity patches within the mafic bodies may represent fluid-filled zones that act as asperity zones and along which large earthquakes might nucleate. A velocity decrease at 62–77 km, covering an area of 120 km $\times$ 80 km, as revealed by receiver function analysis was attributed to the updoming of the asthenosphere or/and the presence of patches of partial melts beneath the central Kachchh rift zone. These may provide favorable circumstances for eclogitization and release of compressed carbon dioxide or fluids that accumulate in some pockets and facilitate occurrence of earthquakes.

We propose that large crustal stresses associated with ongoing uplift, the presence of intrusive mafic bodies, fault intersection, marked lateral variation in crustal thickness, and related sub-crustal thermal anomalies are accumulating in the heterogeneous causative fault of the 2001 mainshock. These stresses are mainly concentrated in the denser and stronger lower crust (at 14–34 km depths) beneath the Kachchh rift zone, within which most of the earthquakes nucleate along the fluid-filled fractured low-velocity zones.

Acknowledgements

A thorough review and numerous suggestions by Pradeep Talwani have tremendously improved the manuscript. Prantik Mandal is grateful to the Director, NGRI, for support and permission to publish this work. The Government of Gujarat and Ministry of Earth-Sciences, New Delhi, supported this work. Girish Kothyari drafted some of the figures.

References

Antolik, M., and Dreger, D. S. (2003). Rupture process of the 26 January 2001 M_w 7.6 Bhuj, India, earthquake from teleseismic broadband data. *Bulletin of the Seismological Society of America*, 93, 1235–1248.

Baker, W. E. (1846). Remarks on the Alla Bund and on the drainage of the Eastern part of the Sind Basin. *Transactions of the Bombay Geographical Society*, 7, 186–188.

Bilham, R. (1999). Slip parameters for the Rann of Kachchh, India, 16 June 1819, earthquake, quantified from contemporary accounts. In *Coastal Tectonics*, ed. I. S. Stewart and C. Vita-Finzi, Geological Society, London, Special Publication, 146, pp. 295–318.

Bisht, R. S. (1997). Dholavira excavations: 1990–94, Facets of Indian Civilization: Essay in Honour of Prof. B. B. Lal, ed. J. P. Joshi, New Delhi: Aryan Books, International, 1, 107–120.

Bisht, R. S. (2011). Major earthquake occurrences in archaeological strata of Harappan settlement at Dholavira (Kachchh, Gujarat). *International Symposium on the 2001 Bhuj Earthquake and Advances in Earthquake Science, AES 2011*, ISR, Gandhinagar, Gujarat, S16_IGCP-11, pp. 112–113.

Biswas, S. K. (1987). Regional framework, structure and evolution of the western marginal basins of India. *Tectonophysics*, 135, 302–327.

Biswas, S. K. (2005). A review of structure and tectonics of Kutch Basin, Western India, with special reference to earthquakes. *Current Science*, 88(10), 15.

Biswas, S. K., and Khattri, K. N. (2003). Structure and tectonics of Kutch Basin, Western India, with special reference to earthquake. *Journal of the Geological Society of India*, 61, 626–629.

Bott, M. H. P., and Dean, D. S. (1973). Stress diffusion from plate boundaries. *Nature*, 243, 339–341.

Choudhury, P., Dumka, R. K., Rastogi, B. K., Sreejith, K. M., and Majumdar, T. J. (2012). Interferometric Synthetic Aperture Radar (INSAR) Studies by ISRO and ISR. *ISR Annual Report 2011–12*, www.isr.gujarat.gov.in, pp. 30–32.

Choudhury, P., Catherine, J. K., Gahalaut, V. K., *et al*. (2013a). Post-seismic deformation associated with the 2001 Bhuj earthquake. *Natural Hazards*, 65(2), 1109–1118, doi:10.1007/s11069–012–0191–8.

Choudhury, P., Roy, K. S., and Rastogi, B. K. (2013b). Strain analysis in Kachchh and Saurashtra region using GPS data. *ISR Annual Report, 2012–13*, www.isr.gujarat.gov.in, pp. 46–48.

Desai, A. G., Markwick, A., Vaselli, O., and Downes, H. (2004). Granulite and pyroxenite xenoliths from the Deccan trap: insight into the nature and composition of the lower lithosphere beneath cratonic India. *Lithos*, 78, 263–290.

Deverchere, J., Petit, C., Gileva, N., *et al*. (2001). Depth distribution of earthquakes in the Baikal rift system and its implications for the rheology of the lithosphere. *Geophysical Journal International*, 146, 714–730.

Dumka, R. K., and Rastogi, B. K. (2013). Crustal strain in the rupture zone of 2001 Bhuj earthquake. *ISR Annual Report 2012–13*, isr.gujarat.gov.in, pp. 45–46.

Dura-Gomez, I., and Talwani, P. (2009). Finding faults in the Charleston Area, South Carolina: 1. *Seismological Data, Seismological Research Letters*, 80, 883–900.

Gangopadhyay, A., and Talwani, P. (2003). Symptomatic features of intraplate earthquakes. *Seismological Research Letters*, 74 (6), 863–883.

Gao, S. S., Kelly, H., Liu, H., and Chen, C. (2004). Significant crustal thinning beneath the Baikal rift zone: new constraints from receiver function analysis. *Geophysical Research Letters*, 31, L20610 1–4.

Gowd, T. N., Srirama Rao, S. V., and Gaur, V. K. (1992). Tectonic stress field in the Indian subcontinent. *Journal of Geophysical Research*, 97, 11,879–11,888.

Gupta, H. K., Harinarayana, T., Kousalya, M., *et al*. (2001). Bhuj earthquake of 26 January, 2001. *Journal of the Geological Society of India*, 57, 275–278.

John, T., and Schenk, V. (2006). Interrelations between intermediate-depth earthquakes and fluid flow within subducting oceanic plates: constraints from eclogite facies pseudotachylytes. *Geology*, 34, 557–560.

Johnston, A. C. (1994). Seismotectonic interpretations and conclusions from the stable continental regions. In *The Earthquakes of Stable Continental Regions: Vol. 1, Assessment of Large Earthquake Potential*, ed. J. F. Schneider. Palo Alto, CA: Electric Power and Research Institute, pp. 20–40.

Johnston, A. C. (1996). Seismic moment assessment of earthquakes in stable continental regions. *Geophysical Journal International*, 124, 381–414.

Karmalkar, N. R., Griffin, W. L., and O'Reilly, S. Y. (2000). Ultramafic xenoliths from Kutch, northwest India: plume related mantle samples? *International Geological Review*, 42, 416–444.

Karmalkar, N. R., Kale, M. G., Duraiswami, R. A., and Jonalgadda, M. (2008). Magma underplating and storage in the crust-building process beneath the Kutch region, NW India. *Current Science*, 94, 1582–1588.

Kato, A., Kurashimo, E., Igarashi, T., *et al*. (2009). Reactivation of ancient rift systems triggers devastating intraplate earthquakes. *Geophysical Research Letters*, 36, L05301, 1–5, doi: 10.1029/2008GL036450.

Kovach, R. L., Grijalva, K., and Nur, A. (2010). Earthquakes and civilizations of the Indus valley: a challenge for archaeoseismology. In *Ancient Earthquakes*, ed. M. Sintubin *et al.* Geological Society of America Special Paper 471, pp. 119–127.

Kruger, F., Scherbaum, F., Rosa, J. W. C., *et al*. (2002). Crustal and upper mantle structure in the Amazon region (Brazil) determined with broadband mobile stations. *Journal of Geophysical Research*, 107(B10), ESE 1711–1712.

Kumar, P., Tewari, H. C., and Khandekar, G. (2000). An anomalous high velocity layer at shallow crustal depths in the Narmada zone, India. *Geophysical Journal International*, 142, 95–107.

Liu, L., and Zoback, M. D. (1997). Lithospheric strength and intraplate seismicity in the New Madrid seismic zone. *Tectonics*, 16(4), 585–595.

Malik, J. N., Morino, M., Mishra, P., Bhuiyan, C., and Kaneko, F. (2008). First active fault exposure identified along Kachchh mainland fault: evidence from trench extraction near Lodai village, Gujarat, western India. *Journal of the Geological Society of India*, 71, 201–208.

Mandal, P. (2008). Stress rotation in the Kachchh rift zone, Gujarat, India. *Pure and Applied Geophysics*, 165, 1307–1324.

Mandal, P. (2009). Crustal shear wave splitting in the epicentral zone of the 2001 M_w 7.7 Bhuj earthquake, Gujarat, India. *Journal of Geodynamics*, 47, 246–258.

Mandal, P. (2010). Crustal and lithospheric thinning beneath the seismogenic Kachchh rift zone, Gujarat (India): its implications toward the generation of the 2001 Bhuj earthquake sequences. *Journal of Asian Earth Sciences*, doi. 10.1016/j.jseaes.2010.08.012.

Mandal, P. (2011). Upper mantle seismic anisotropy in the intra-continental Kachchh rift zone, Gujarat, India. *Tectonophysics*, 509, 81–92.

Mandal, P. (2012a). Passive-source seismic imaging of the crust and upper mantle beneath the 2001 M_w 7.7 Bhuj earthquake region, Gujarat, India. *Bulletin of the Seismological Society of America*, 102, 252–266.

Mandal, P. (2012b). Seismogenesis of the uninterrupted occurrence of the aftershock activity in the 2001 Bhuj earthquake zone, Gujarat, India, during 2001–2010. *Natural Hazards*, 65, 1063–1083.

Mandal, P., and Chadha, R. K. (2008). Three-dimensional velocity imaging of the Kachchh seismic zone, Gujarat, India. *Tectonophysics*, 452, 1–16.

Mandal, P., and Horton, S. (2007). Relocation of aftershocks, focal mechanisms and stress inversion: implications toward the seismo-tectonics of the causative fault zone of M_w 7.6 2001 Bhuj earthquake (India). *Tectonophysics*, 429, 61–78.

Mandal, P., and Pandey, O. P. (2010). Relocation of aftershocks of the 2001 Bhuj earthquake: a new insight into seismotectonics of the Kachchh seismic zone, Gujarat, India. *Journal of Geodynamics*, 49, 254–260.

Mandal, P., and Pujol, J. (2006). Seismic imaging of the aftershock zone of the 2001 M_w 7.7 Bhuj earthquake, India. *Geophysical Research Letters*, 33, L05309, 1–4.

Mandal, P., and Rastogi, B. K. (2005). Self-organized fractal seismicity and b-value of aftershocks of 2001 Bhuj earthquake in Kutch (India). *Pure and Applied Geophysics*, 162, 53–72.

Mandal, P., Rastogi, B. K., Satyanarayana, H. V. S., and Kousalya, M. (2004a). Results from local earthquake velocity tomography: implications toward the source process involved in generating the 2001 Bhuj earthquake in the lower crust beneath Kachchh (India). *Bulletin of the Seismological Society of America*, 94(2), 633–649.

Mandal, P., Jainendra, S., Joshi, S. K., Bhunia, R., and Rastogi, B. K. (2004b). Low coda-Qc in the epicentral region of the 2001 Bhuj earthquake of M_w 7.7. *Pure and Applied Geophysics*, 161, 1635–1654.

Mandal, P., Chadha, R. K., Raju, I. P., *et al*. (2007). Coulomb static stress variations in the Kachchh, Gujarat, India: implications for the occurrences of two recent earthquakes ($M_w = 5.6$) in the 2001 Bhuj earthquake region. *Geophysical Journal International*, 169, 281–285.

Mandal, P., Satyamurthy, C., and Raju, I. P. (2009). Iterative de-convolution of the local waveforms: characterization of the seismic sources in Kachchh, India. *Tectonophysics*, 478, 143–157.

Manglik, A., and Singh, R. N. (2002). Thermomechanical structure of the central Indian shield: constraints from deep crustal seismicity. *Current Science*, 82, 1151–1157.

McClay, K., and Bonora, M. (2001). Analog models of restraining stop-overs in strike-slip fault systems. *American Association of Petroleum Geologists Bulletin*, 85, 233–260.

Mechie, J., Keller, G. R., Prodehl, C., *et al*. (1994). Crustal structure beneath the Kenya rift from axial profile data. In *Crustal and Upper Mantle Structure of the Kenya Rift*, ed. C. Prodehl, G. R. Keller, and M. Khan. *Tectonophysics*, 236, 179–199.

Miller, S. A., Collettni, C., Chlaraluce, L., *et al*. (2004). Aftershocks driven by a high pressure CO_2 source at depth. *Nature*, 427, 724–727.

Mishra, O. P., and Zhao, D. (2003). Crack density, saturation rate and porosity at the 2001 Bhuj, India, earthquake hypocenter: a fluid-driven earthquake. *Earth and Planetary Science Letters*, 212, 393–405.

Mogi, K. (1968). Migration of seismic activity. *Bulletin of the Earthquake Research Institute, University of Tokyo*, 46, 53–74.

Mohan, K. (2013). Identification of Kachchh Mainland fault and South Wagad fault from magnetotellurics. *ISR Annual Report 2012–13*, pp. 31–32, www.isr.gujarat.gov.in.

Mooney, W. D., and Christensen, N. I. (1994). Composition of the crust beneath the Kenya Rift. *Tectonophysics*, 236, 391–408.

Mooney, W. D., Andrews, M. C., Ginzburg, A., Peters, D. A., and Hamilton, R. M. (1983). Crustal structure of the northern Mississippi embayment and a comparison with other continental rift zones. *Tectonophysics*, 94, 327–348.

Morino, M., Malik, J. N., Mishra, P., Bhuiyan, C., and Kaneko, F. (2008a). Active fault traces along Bhuj fault and Katrol hill fault, and trenching survey at Wandhay, Kachchh, Gujarat, India. *Journal of Earth System Science*, 117(3), 181–188.

Morino, M., Malik, J. N., Gadhavi, M. S., *et al*. (2008b). Active low-angle reverse fault and wide quaternary deformation identified in Jhura Trench across Kachchh Mainland Fault, Kachchh, Gujarat, India. *Journal of Active Fault Research, Japan*, 29, 71–77.

Mukherjee, S. M. (1942). Seismological features of the Satpura earthquake of the 14th March 1938. *Proceedings of Indian Academy of Sciences*, 16, 167–175.

Nagabhushan Rao, Ch. (2012). Moment tensor and fault mechanism solutions. *ISR Annual Report 2011–12*, pp. 10–11, www.isr.gujarat.gov.in.

Nyblade, A. A., and Langston, C. A. (1995). East African earthquakes below 20 km depth and their implications for crustal structure. *Geophysical Journal International*, 121, 49–62.

Padhy, S., and Crampin, S. (2006). High pore-fluid pressures at Bhuj, inferred from 90°-flips in shear-wave polarizations. *Geophysical Journal International*, 164, 370–376.

Pandey, O. P., Chandrakala, K., Parthasarathy, G., Reddy, P. R., and Koti Reddy, G. (2009). Upwarped high velocity mafic crust, subsurface tectonics and causes of intra plate Latur-Killari (M 6.2) and Koyna (M 6.3) earthquakes, India: a comparative study. *Journal of Asian Earth Sciences*, 34, 781–795.

Paul, J., Burgmann, R., Gaur, V. K., *et al*. (2001). The motion and active deformation of India. *Geophysical Research Letters*, 28(4), 647–651.

Paul, D. K., Ray, A., Das, B., Patil, S. K., and Biswas, S. K. (2008). Petrology, geochemistry and paleomagnetism of the earliest magmatic rocks of Deccan Volcanic Province, Kutch, Northwest India. *Lithos*, 102(1–2), 237–259.

Pratt, T. L. (2012). Kinematics of the New Madrid seismic zone, central United States, based on stepover models. *Geology*, 40, 371–374.

Prodehl, C., Keller, G. R., and Khan, M. A. (1994). Crustal and upper mantle structure of the Kenya rift. *Tectonophysics*, 236, 483.

Rajendran, C. P. (2000). Using geological data for earthquake studies: a perspective from peninsular India. *Current Science*, 79(9), 1251–1258.

Rajendaran, C. P., and Rajendaran, K. (1998). Characteristics of the 1997 Jabalpur earthquake and their bearing on its mechanism. *Current Science*, 74, 168–177.

Rajendran, C. P., and Rajendran, K. (2001). Characteristics of deformation and past seismicity associated with the 1819 Kutch earthquake, northwestern India. *Bulletin of the Seismological Society of America*, 91(3), 407–426.

Rajendran, K., and Rajendran, C. P. (2002). Historical constraints on previous seismic activity and morphologic changes near the source zone of the 1819 Rann of Kachchh earthquake: further light on the penultimate event. *Seismological Research Letters*, 73, 470–479.

Rajendran, K., and Rajendran, C. P. (2003). Seismogenesis in the stable continental regions and implications for hazard assessment: two recent examples from India. *Current Science*, 85(7), 896–903.

Rastogi, B. K. (2001). Ground deformation study of M_w 7.7 Bhuj earthquake of 2001. *Episodes*, 30(1), 160–165.

Rastogi, B. K., Gupta, H. K., Mandal, P., *et al*. (2001). The deadliest stable continental region earthquake that occurred near Bhuj on 26 January 2001. *Journal of Seismology*, 5, 609–615.

Rastogi, B. K., Choudhury, P., Dumka, R., Sreejith, K. M., and Majumdar, T. J. (2012). Stress pulse migration by viscoelastic process for long-distance delayed triggering of shocks in Gujarat, India, after the 2001 M_w 7.7 Bhuj earthquake. In *Extreme Events and Natural Hazards: The Complexity Perspective*, ed. A. S. Sharma, A. Bundle, V. P. Dimri and D. N. Baker. Geophysical Monograph Series, 196, AGU, Washington, D.C., pp. 63–73, doi:10.10.1029/GM196.

Rastogi, B. K., Kumar, S., Aggrawal, S. K. (2013a). Seismicity of Gujarat. *Natural Hazard*, 65(2), 1027–1044.

Rastogi, B. K., Aggrawal, S. K., Rao, N., and Choudhury, P. (2013b). Triggered/migrated seismicity due to the 2001 M_w 7.6 Bhuj earthquake, Western India. *Natural Hazard*, 65(2), 1085–1107.

Ray, A., Patil, S. K., Paul, D. K., *et al*. (2006). Petrology, geochemistry and magnetic properties of Sadara Sill: evidence of rift related magmatism from Kutch Basin, Northwest India. *Journal of Asian Earth Sciences*, 27, 907–921.

Reddy, C. D., and Sunil, P. S. (2008). Post seismic crustal deformation and strain rate in Bhuj region, western India, after the 2001 January 26 earthquake. *Geophysical Journal International*, 172, 593–606.

Russ, D. P. (1982). Style and significance of surface deformation in the vicinity of New Madrid, Missouri: investigations of the New Madrid, Missouri, earthquake region. In *Investigations of the New Madrid Earthquake Region*, ed. F. A. McKeown and L. C. Pakiser, U.S. Geological Survey Professional Paper 1236, pp. 95–114.

Sarkar, D., Sain, K., Reddy, P. R., Catchings, R. D., and Mooney, W. D. (2007). Seismic-reflection images of the crust beneath the 2001 $M = 7.7$ Kutch (Bhuj) epicentral region, western India. In *Continental Intraplate Earthquakes: Science, Hazard, and Policy Issues*, ed. S. Stein and S. Mazzotti, Geological Society of America Special Paper 425, pp. 319–327.

Savage, J. C. (1971). A theory of creep waves propagating along a transform fault. *Journal of Geophysical Research*, 76(8), 1954–1966.

Scholz, C. H. (1977). A physical interpretation of the Haicheng earthquake prediction. *Nature*, 267, 121–124.

Segall, P., and Pollard, D. D. (1980). Mechanics of discontinuous faults. *Journal of Geophysical Research*, 85, 4,337–4,350.

Sen, G., Bizimis, M., Das, R., *et al*. (2009). Deccan plume, lithospheric rifting, and volcanism in Kutch, India. *Earth and Planetary Science Letters*, 277, 101–111.

Sharma, B. S., Chopra, S., Rao, K. M., Gupta, A. K., and Rastogi, B. K. (2008). Attenuation and heterogeneity. *ISR Annual Report 2007–8*, pp. 11–14, www.isr.gujarat.gov.in.

Sibson, R. H. (1986). Rupture interaction with fault jogs. In *Earthquake Source Mechanics*, ed. S. Das, J. Boatwright, and C. H. Scholz, AGU Geophysical Monograph 37, Maurice Ewing Series 6, pp. 157–167.

Singh, B. P., ed. (1996). *Indian Archeology 1991–1992: A Review*, New Delhi: Archeological Survey of India.

Singh, S. K., Dattatrayam, R. S., Shapiro, N. M., *et al.* (1999). Crustal and upper mantle structure of Peninsular India and source parameters of the May 21, 1997, Jabalpur earthquake [$M_w = 5.8$]: results from a new regional broad-band network. *Bulletin of the Seismological Society of America*, 89, 1632–1641.

Singh, A. P., Mishra, O., Rastogi, B. K., and Kumar, D. (2011). 3-D seismic structure of the Kachchh, Gujarat, and its implications for the earthquake hazard mitigation. *Natural Hazards*, 57, 1–23.

Singh, A. P., Mishra, O. P., Yadav, R. B. S., and Kumar, D. (2012). New insight into crustal heterogeneity beneath the 2001 Bhuj earthquake region of Northwest India and its implications for rupture initiations. *Journal of Asian Earth Sciences*, 48, 31–42, doi: 10.1016/j.jseaes.2011.12.020.

Singh, A. P., Mishra, O. P., Rastogi, B. K., and Kumar, S. (2013). Crustal heterogeneities beneath the 2011 Talala, Saurashtra earthquake, Gujarat, India source zone: seismological evidence for neo-tectonics. *Journal of Asian Earth Sciences*, 62, 672–684.

Sreejith, K. M., and Rastogi, B. K. (2013). Interferometric Synthetic Aperture Radar (INSAR) studies in Kachchh by ISRO and ISR. *ISR Annual Report 2012–13*, pp. 49–51, www.isr.gujarat.gov.in.

Talwani, P., Chen, L., and Kalpana, G. (2007). Seismogenic permeability, Ks. *Journal of Geophysical Research*, 112, B07309, doi:10.1029/2006JB004665.

Wang, Z., and Zhao, D. (2006). Seismic evidence for the influence of fluids on the 2005 west off Fukuoka prefecture earthquake in southwest Japan. *Physics of the Earth and Planetary Interiors*, 155, 313–324.

Wilson, D., Aster, R., and the RISTRA Team (2003). Imaging crust and upper mantle seismic structure in the southwestern United States using teleseismic receiver functions. *Leading Edge*, 22, 232–237.

Zhao, D., Kanamori, H., Negishi, H., and Wiens, D. (1996). Tomography of the source area of the 1995 Kobe earthquake: evidence for fluids at the hypocenter. *Science*, 274, 1891–1894.